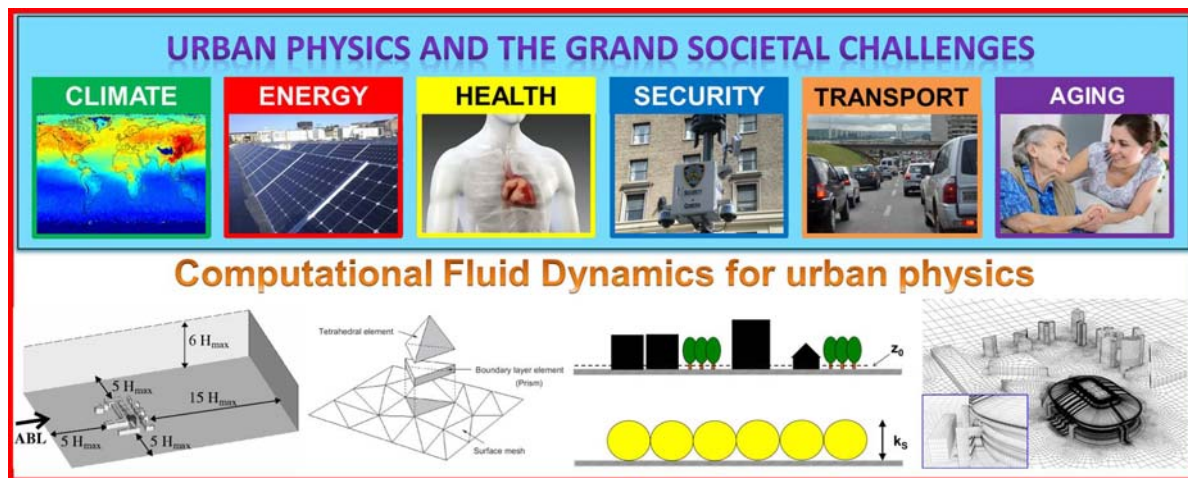


Computational Fluid Dynamics for Urban Physics: Importance, scales, possibilities, limitations and ten tips and tricks towards accurate and reliable simulations

Bert Blocken *

*Building Physics and Services, Department of the Built Environment, Eindhoven University of Technology,
P.O. box 513, 5600 MB Eindhoven, the Netherlands, b.j.e.blocken@tue.nl
Building Physics Section, Department of Civil Engineering, Leuven University, Kasteelpark Arenberg 40 - bus
2447, 3001 Leuven, Belgium*

Graphical abstract



Highlights

- Review and position paper on Computational Fluid Dynamics for urban physics
- Urban physics to address urban grand challenges climate, energy, health, security, transport, aging
- Spatial scales: meteorological macroscale, mesoscale, microscale, building, component and human scale
- CFD for urban physics: mainly RANS, not LES, for two reasons: computational cost and best practice guidelines
- Ten tips and tricks towards accurate and reliable CFD simulations

* **Corresponding author:** Bert Blocken, Building Physics and Services, Department of the Built Environment, Eindhoven University of Technology, P.O. Box 513, 5600 MB Eindhoven, the Netherlands. *E-mail address:* b.j.e.blocken@tue.nl

Computational Fluid Dynamics for Urban Physics: Importance, scales, possibilities, limitations and ten tips and tricks towards accurate and reliable simulations

Bert Blocken *

*Building Physics and Services, Department of the Built Environment, Eindhoven University of Technology,
P.O. box 513, 5600 MB Eindhoven, the Netherlands, b.j.e.blocken@tue.nl
Building Physics Section, Department of Civil Engineering, Leuven University, Kasteelpark Arenberg 40 - bus
2447, 3001 Leuven, Belgium*

Abstract

Urban physics is the science and engineering of physical processes in urban areas. It basically refers to the transfer of heat and mass in the outdoor and indoor urban environment, and its interaction with humans, fauna, flora and materials. Urban physics is a rapidly increasing focus area as it is key to understanding and addressing the grand societal challenges climate change, energy, health, security, transport and aging. The main assessment tools in urban physics are field measurements, full-scale and reduced-scale laboratory measurements and numerical simulation methods including Computational Fluid Dynamics (CFD). In the past 50 years, CFD has undergone a successful transition from an emerging field into an increasingly established field in urban physics research, practice and design. This review and position paper consists of two parts. In the first part, the importance of urban physics related to the grand societal challenges is described, after which the spatial and temporal scales in urban physics and the associated model categories are outlined. In the second part, based on a brief theoretical background, some views on CFD are provided. Possibilities and limitations are discussed, and in particular, ten tips and tricks towards accurate and reliable CFD simulations are presented. These tips and tricks are certainly not intended to be complete, rather they are intended to complement existing CFD best practice guidelines on ten particular aspects. Finally, an outlook to the future of CFD for urban physics is given.

Keywords: Computational Fluid Dynamics; CFD; Urban physics; Building physics; Fluid mechanics; Urban environment

1. Introduction

*“Scientists study the world as it is; engineers create the world that has never been.”*¹

Urban physics is the science and engineering of physical processes in urban areas. It basically refers to the transfer of heat and mass in the outdoor and indoor urban environment, but also their interaction with humans, fauna, flora and materials. From the human point of view, the main aim of urban physics is to provide a healthy, comfortable and sustainable outdoor and indoor built environment taking into account climatic, energetic and economic constraints. As such, it is strongly related to the grand societal challenges climate (change), energy, health (including comfort), security, transport and aging.

In urban physics, science and engineering are strongly intertwined. Urban physics is an applied discipline. It is also inherently multidisciplinary. In its narrowest sense, it has its roots in building engineering/building physics, civil engineering and architectural engineering, and it is strongly based on mathematics, physics and chemistry. However, urban physics is a rapidly expanding discipline. The main reasons are the increasing urbanization and the fact that urban physics is key to understanding and addressing the grand societal challenges pertaining to this increasing urbanization. Because of the increasing importance of urban physics, the past decades have seen a tremendous growth of the urban physics community. Scientists and engineers from disciplines that traditionally did not have an explicit focus or even no focus at all on buildings and urban areas, are now shifting the focus of the work in their discipline to buildings and urban areas. As a result, in this broader sense, urban physics is practiced in many more engineering disciplines, from mechanical and electrical

* **Corresponding author:** Bert Blocken, Building Physics and Services, Department of the Built Environment, Eindhoven University of Technology, P.O. Box 513, 5600 MB Eindhoven, the Netherlands. *E-mail address:* b.j.e.blocken@tue.nl

¹ Theodore von Kármán (1881 – 1963), Hungarian-American mathematician, physicist and aerospace engineer.

engineering over computer engineering and chemical engineering to urban planning and design, and it also draws from disciplines such as meteorology, human thermophysiology, psychology and material science.

Urban physics encompasses processes acting at a wide range of spatial and temporal scales, which will be addressed further in section 3 of this paper. The spatial scales that are the main focus in urban physics are the (meteorological) microscale and the building scale, where the former is defined as the scale of atmospheric motions with Lagrangian Rossby numbers greater than 200 or spatial scales of 2 km or less [1]. At these scales, many problems in urban physics can be tackled by one of three approaches, or a combination of these: (1) field measurements, (2) full-scale or reduced-scale wind-tunnel measurements; and (3) numerical simulation. In terms of numerical simulation, especially at the meteorological microscale, the main approach is Computational Fluid Dynamics (CFD).

Deciding which approach is most appropriate for a given problem is not always straightforward, as each approach has specific advantages and disadvantages. The main advantage of field measurements is that they are able to capture the real complexity of the problem under study. Important disadvantages however are that they are not fully controllable due to – among others – the inherently variable meteorological conditions, that they are not possible in the design stage of a building or urban area and that usually only point measurements are performed. The main advantages of wind-tunnel measurements are the large degree of control over the boundary conditions and test conditions and the fact that buildings, urban areas and their components can be evaluated in the design stage. However, as in field measurements, also in wind-tunnel measurements, generally only point measurements are performed. Techniques such as Particle Image Velocimetry (PIV) and Laser-Induced Fluorescence (LIF) in principle allow planar or even full 3D data to be obtained, but the cost is considerably higher and application for complicated geometries can be hampered by laser-light shielding by the obstructions constituting the model, e.g. in case of an urban model consisting of many buildings. Another potential disadvantage of wind-tunnel testing is the required adherence to similarity criteria when testing at reduced scale. This can be a problem for, e.g., multiphase flow problems and buoyant flows. Examples are the transport and deposition of sand, dust, rain, hail, and snow, and buoyancy-driven natural ventilation and pollutant dispersion studies.

Numerical modeling with CFD can be a powerful alternative because it can avoid some of these limitations. It can provide detailed information on the relevant flow variables in the whole calculation domain (“whole-flow field data”), under well-controlled conditions and without similarity constraints. However, the accuracy of CFD is an important matter of concern. Care is required in the geometrical implementation of the model, in grid generation, in selection of proper solution strategies and in interpretation of the results. Selection of proper solution strategies includes choices between the steady Reynolds-averaged Navier-Stokes (RANS) approach, the unsteady RANS (URANS) approach, Large Eddy Simulation (LES) or hybrid URANS/LES, choices between different turbulence models, discretization schemes, etc. In addition, numerical and physical modeling errors need to be assessed by solution verification and validation studies. CFD validation in turn requires high-quality experimental data to be compared with the simulation results.

This paper focuses on CFD for urban physics. It consists of two parts. In the first part, the importance of urban physics related to the grand societal challenges is described (section 2), after which the spatial and temporal scales in urban physics and the associated model categories are outlined (section 3). In the second part, based on a brief theoretical background, some views on CFD are provided. Possibilities and limitations are described (section 4), and in particular, ten tips and tricks towards accurate and reliable CFD simulations are presented (section 5). These tips and tricks are certainly not intended to be complete, rather they are intended to complement existing CFD best practice guidelines on ten particular aspects. Finally, an outlook to the future of CFD for urban physics is given (section 6).

2. Importance: grand societal challenges and application areas

“One thing I have learned in a long life: that all our science, measured against reality, is primitive and childlike - and yet it is the most precious thing we have.”²

2.1. Grand societal challenges

2.1.1. Urbanization

The grand societal challenges include climate, energy, health, security, transport and aging, many of which are interrelated and all of which are increasingly present in urban areas due to the continuing urbanization in the past decades. Urbanization is defined as a shift of the population from rural areas to urban areas. The 2014 Revision of World Urbanization Prospects by the United Nations (UN) mentions that currently and globally,

² Albert Einstein (1879 – 1955), German theoretical physicist.

more people live in urban areas than in rural areas [2]. While in 1950 only 30 % of the world's population was urban, in 2014, this number has risen to 54 %, and it is expected to reach 66 % by 2050 [2] (Fig. 1). All regions are expected to urbanize further over the coming decades [2]. The UN state that urbanization is a major concern as this trend is *“changing the landscape of human settlement, with significant implications for living conditions, the environment and development in different parts of the world”* [3]. Indeed, while urbanization is generally associated with and driven by advantages such as improved opportunities, services and reduced costs for education, health, work, transport and housing, mainly resulting from centralization, it also entails considerable problems and challenges in terms of climate, energy, health, security, transport/mobility and aging, some of which are further explained below. The remainder of this section is not intended to be complete: the focus is on some main aspects of these challenges related to urban physics.

2.1.2. Climate change

In its Fifth Assessment Report, the International Panel for Climate Change (IPCC) states that human influence on the climate system is clear and that, mainly due to economic and population growth, the anthropogenic greenhouse gas emissions are now the highest in history [4]. It warns that *“the continued emission of greenhouse gases will cause further global warming and long-lasting changes in all components of the climate system, increasing the likelihood of severe, pervasive and irreversible impacts for people and ecosystems”* [4]. Unfortunately, emissions are expected to rise even further, by 20% to 2040, ensuring continued climate change [4]. Mitigation of climate change and adaptation to climate change are urgently needed. Mitigation refers to limiting climate change by substantial and sustained reductions in the emission of greenhouse gases. But even if mitigation would be immediate and complete, still climate change would continue to some extent, due to the current presence of greenhouse gases in the atmosphere. Therefore, also adaptation to climate change is needed, which refers to *“anticipating the adverse effects of climate change and taking appropriate action to prevent or minimize the damage they can cause, or taking advantage of opportunities that may arise”* [5].

Adverse effects of climate change that are particularly relevant for urban areas are sea-level rise and coastal flooding, more intense and frequent heat waves, more intense and frequent precipitation events, pluvial flooding, drought and increased air pollution. The combination of urbanization and climate change is particularly problematic. On the one hand, urbanization increases the exposure of the population to the effects of climate change, such as heat waves, precipitation events, flooding and air pollution. On the other hand, urbanization is associated with larger energy demand and energy consumption, and hence more greenhouse gas emissions. This is due to the growth of cities and the emergence of new cities, but also due to the fact that city residents tend to consume more energy than their rural counterparts, so they therefore emit more CO₂ per capita [6]. The International Energy Agency (IEA) states that the bulk of the increase in global energy-related CO₂ emissions is expected to come from cities, and that their share is expected to rise from 71% in 2006 to 76% in 2030 as a result of continued urbanization [6].

The adverse effects of heat waves and high temperatures on human morbidity and mortality and energy use in buildings have been investigated in various studies about climate change [7-9] and heat waves [10-12]. Fig. 2, reproduced from a study by Garssen et al. [11], illustrates the relation between the average weekly maximum outdoor air temperature in the heat-wave period in 2003 and the number of deaths in the Netherlands for each of those weeks. The figure shows that higher average weekly maximum temperatures result in a higher number of deaths. Since people spend around 90% of their time indoors [13], the adaptation of urban areas and buildings to the predicted climate change is important to protect people against excessive exposure to high indoor air temperatures. Traditional electrical cooling systems should be avoided, as they reduce the indoor temperature at the expense of further increasing the outdoor temperature, which in turn would give rise to an increased need to use such electrical cooling systems to keep indoor temperatures sufficiently low – a vicious circle. In urban areas, the impacts of heat waves are aggravated by the urban heat island effect (UHI), which refers to urban areas being significantly warmer than their rural surroundings, mainly because urban areas retain more heat [14-19]. The main causes of the UHI are schematically depicted in Figure 3.

2.1.3. Energy

The global energy system is under pressure [20]. Due to the growing world population and economy, the global energy demand is expected to have increased by 37% in 2040 in the IEA New Policies Scenario³, and the energy supply mix is expected to consist of four almost equal parts: oil, gas, coal and low-carbon sources

³ The scenario in the World Energy Outlook that takes account of broad policy commitments and plans that have been announced by countries, including national pledges to reduce greenhouse-gas emissions and plans to phase out fossil-energy subsidies, even if the measures to implement these commitments have yet to be identified or announced. This broadly serves as the IEA baseline scenario (from [21]).

[20]. This implies that CO₂ emissions will continue to rise, as will the related risks of climate change. In 2006, about two-thirds of the world's energy (estimated at 7900 Mtoe) was consumed in urban areas [6]. Due to the increasing urbanization, it is expected that by 2030, urban areas will consume 73% of the world's energy (estimated at 12,400 Mtoe) [6]. In 2014, buildings were stated to use about 40% of the global energy and to be responsible for about one-third of the greenhouse gas emissions [22].

Energy efficiency and renewable energy systems are essential instruments to reduce the pressure on the global energy system as well as on the global climate system. Given the concentration of energy consumption in urban areas and the high energy consumption by buildings, energy efficiency is particularly relevant in urban areas and for buildings. Renewable energy systems refer to wind energy, solar energy, hydro-electric energy, tidal energy, geothermal energy and biomass. They are increasingly applied inside and outside urban areas to provide energy to these areas. Application of these systems inside urban areas has the advantage that then the energy is produced where it is consumed. Application outside urban areas will require transport of energy and hence increased costs (and increased consumption of energy).

2.1.4. Health

Urbanization provides many opportunities for better health but it also entails considerable challenges. The World Health Organization (WHO) distinguishes three health threats for cities [23,24]: (1) infectious diseases like HIV/AIDS, TB, pneumonia, diarrhoeal diseases; (2) non-communicable diseases like asthma, heart disease, cancer and diabetes; and (3) violence and injuries, including road traffic injuries. A wide range of health determinants can be held responsible for these threats. Those most closely related to urban physics include heat stress, outdoor and indoor air pollution, wind danger and noise. According to the WHO, air pollution killed about 1.2 million people worldwide in 2004, the largest part due to fine particulate matter from vehicle and industrial fuel combustion [25]. Wind danger refers to high wind speed at pedestrian level around buildings that can lead to injuries or death; it will be discussed in section 2.2.

A very worrying trend and consequence of urbanization is the increasing concentration of poverty in cities, while in the past centuries, poverty was largest in scattered rural areas [25]. Poverty, deprivation and inferior social and living conditions are often strongly related to poor health. In many countries, urbanization has developed and continues to develop too fast for governments to build the necessary infrastructure for healthy living conditions [25].

Urbanization itself is also held responsible for amplifying adverse trends related to health: climate change and the increase of chronic diseases [25]. As mentioned earlier, city inhabitants are especially vulnerable to the consequences of climate change, such as heat waves, increased air pollution and rising sea levels [25]. The WHO states five actions to be undertaken to build a healthy and safe urban environment [25]: (1) promoting urban planning for healthy behavior and safety; (2) improving urban living conditions; (3) ensuring participatory urban governance; (4) building inclusive cities that are accessible and age-friendly; (5) making urban areas resilient to emergencies and disasters.

2.1.5. Security

The Institute for Security and Open Methodologies (ISECOM) defines security as “a form of protection where a separation is created between the assets and the threat” [26]. Assets can be persons, infrastructure, houses, organizations, etc., and distinctions are then made in terms of human security, infrastructure security, home security, national and international security, etc. The United Nations Development Program (UNDP) 1994 report introduced the concept of human security, which connects security with people rather than territories [27]. Particular threats to human security were identified in seven areas: economic security, food security, health security, environmental security, personal security, community security and political security. Health security (protection from diseases and injuries) and environmental security (protection from acts of nature, man-made threats in nature and deterioration of the environment) are strongly related to urbanization. Also personal security (protection from physical violence, crime) is connected to urbanization. In terms of urban physics, health security and environmental security are closely linked, in particular concerning protection from heat waves, air pollution, fire, etc.

2.1.6. Transport

Transport refers to the movement of people, goods, etc. from one location to another by road, shipping, aviation and rail. Transport infrastructure and vehicles are key components of urban areas. As transport is closely related to economy and environment, urbanization is generally associated with increased transport infrastructure, services and vehicles. But transport is also a major contributor to air pollution and climate change. Actually, it is the fastest growing emission sector of CO₂ [28]. Global CO₂ emissions increased by

13% from 1990 to 2000, but CO₂ emissions from road transport and aviation each grew by 25% [28]. Therefore, transport efficiency becomes increasingly important. It includes modal shifts, i.e. a transition from air and road to rail and human powered transport, reduction of traffic jams and fuel efficiency. Transport is not only closely related to climate, but also to health and security (traffic-related injuries, air pollution, stress).

2.1.7. Aging

Aging refers to the increase in the number of elderly and their proportion in the world population. The WHO states that between 2000 and 2050, the percentage of the world population older than 60 years will double from about 11 to 22%, and the number of people older than 80 years will almost quadruple [29]. This is mainly caused by the combination of declining birth rates and longer life expectancy. While because of the latter cause, aging can be seen as a success story of our modern society and as proof for efficiency and effectiveness of health care policies and services, it also gives rise to challenges. It imposes the need for long-term care infrastructure such as home nursing, community care, assisted living, stays in hospitals, etc. This infrastructure is primarily developed and concentrated in cities, which causes a shift of the elderly population from rural to urban areas. As such, aging reinforces urbanization, and urbanization – by better health care – reinforces aging. On the other hand, the urbanization-related threats in terms of health and security that were outlined in the previous subsection, are particularly eminent for the elderly portion of the urban population, because they belong to the most vulnerable of our society.

2.2. Urban physics focus areas

The grand societal challenges give rise to and/or are related to a wide range of focus areas in urban physics. These focus areas and their link to the most relevant societal challenges are schematically depicted in Figure 4. Below, they are explained in more detail, and references to some review, overview and position papers on these areas – mainly, but not exclusively, related to CFD modeling – are given.

Climate, climate change and environment are related to urban physics research on outdoor and indoor thermal environment (including heat waves) [19,30-33], pollutant dispersion in urban areas [34-46], pedestrian-level wind conditions around buildings in high wind speed and storm events [30-32,42,47-51], increase of meteorological phenomena such as thunderstorms and downbursts, wind loads on buildings and infrastructure due to meteorological phenomena and high wind speed [52-56], wind loads on vehicles [57], increased intensity and frequency of wind-driven rain and the related problems of rain penetration and deterioration of building facades [33,42,51,58-60], danger and damage due to windborne debris during storms [61-64] and urban and building fire spreading. Note that Building and Environment recently published two Special Issues on climate change in urban areas: “The implications of a changing climate for buildings” in 2012 [65] and “Climate adaptation in cities” in 2015 [66], and one Virtual Special Issue on “CFD simulation of micro-scale pollutant dispersion in the built environment” [45].

Energy is connected to urban physics research on natural ventilation of buildings including ventilative cooling [51,67-77], vehicle aerodynamics in terms of their energy consumption [57,78-81] and on wind energy and solar energy in the built environment [82-88]. Health is represented in research on thermal environment, heat stress, thermal comfort and warning systems for heat waves [19,30-33], urban air quality and pollutant dispersion [34-46], avoidance of wind danger for pedestrians around high-rise buildings [30-32,42,47-51], natural ventilation for indoor air quality [51,67-77] and urban acoustics [89-94]. Security refers to pollutant dispersion and warning systems for toxic accidents and terrorist attacks [34-46], detection and warning for destructive meteorological phenomena, avoidance of occurrence and impacts of windborne debris [61-64] and fire safety in terms of limiting both occurrence and spreading. Transport/mobility requires research on air pollution by traffic [34-46], control of snow drift and accumulation around buildings on roads and other infrastructural elements [95], safety of land, water and air vehicles [57] and reduction of traffic-induced noise [89-94]. Finally, aging is connected to health and comfort for the elderly in our society who are residing in the urban thermal environment [19,30-33], avoidance of wind danger around high-rise buildings and the related (deathly and other) elderly casualties [30-32,42,47-51], and a healthy and comfortable outdoor and indoor acoustic environment [89-94].

While it are these focus areas that are directly related to the grand societal challenges, it should be noted that research in these areas is strongly supported by important basic (or “fundamental”) research efforts in urban physics. Review, overview and position papers on basic research have focused on CFD simulation of the lower part of the atmospheric boundary layer [96-101], on bluff-body aerodynamics, turbulence modeling and numerical techniques in CFD [52,57,96-127] and on verification and validation in CFD for urban physics and wind engineering [96-98,102,128].

3. Spatial and temporal scales and model categories

“δῶς μοι πᾶ στῶ καὶ τὰν γᾶν κινάσω”⁴

In terms of vertical spatial scales, the focus in urban physics is on the lower part of the atmospheric boundary layer (ABL). The ABL is defined as the bottom layer of the troposphere that is in contact with the surface of the Earth [129]. The ABL is highly variable in space and time. Its height ranges from several tens of meter in conditions of strong stable stratification, to several kilometers in conditions of strong unstable stratification or convection. In terms of horizontal spatial scales, the focus in urban physics is mainly – but not exclusively – on the so-called meteorological microscale and the building scale. However, for completeness, this section will address urban physics in its widest sense; it will therefore mention all relevant spatial scales and all related model categories.

Figure 5, adopted from [130] and based on [131], provides an overview of the spatial and temporal scales of atmospheric phenomena. A distinction is made between the meteorological macroscale (or synoptic scale), the mesoscale and the microscale. The American Meteorological Society (AMS) provides the following definitions [1]:

- Macroscale or synoptic scale: the scale of atmospheric motions with a typical range of many hundreds of kilometers, including such phenomena as cyclones and tropical cyclones.
- Mesoscale: the scale of atmospheric phenomena having horizontal scales ranging from a few to several hundred kilometers, including thunderstorms, squall lines, fronts, precipitation bands in tropical and extratropical cyclones, and topographically generated weather systems such as mountain waves and sea and land breezes.
- Microscale: the scale of atmospheric motions with Lagrangian Rossby numbers greater than 200 or spatial scales of 2 km or less.

Figure 5 also indicates which phenomena are directly simulated, implemented as boundary conditions or parameterized in two categories of meteorological models: mesoscale models and microscale models. Microscale meteorological models are generally termed CFD models. In CFD, information from the mesoscale (and implicitly also the macroscale) can be used as boundary conditions. The phenomena that are directly (or better: explicitly) simulated are specific items at the meteorological microscale (e.g. thermals, building wakes, large-scale turbulence), while part of the turbulence is parameterized. Which part of the turbulence is parameterized depends on the CFD approach: LES, hybrid URANS/LES, URANS or steady RANS. In addition to the spatial scales, Figure 5 also provides detailed information on the temporal scales. The very wide range of the spatial and temporal scales indicates the difficulty to study, model and measure atmospheric phenomena.

However, urban physics is not confined to the atmospheric phenomena in Figure 5. A more complete view in terms of extent of spatial scales and the related model categories in urban physics is given in Figure 6. At the macroscale or the synoptic scale and at the mesoscale, the numerical integration of the approximate forms of the governing equations for atmospheric dynamics subject to specified initial conditions is termed Numerical Weather Prediction (NWP) [132-142]. More specifically, models at the mesoscale are also called Mesoscale Meteorological Models (MMM) [137-143]. Microscale meteorological models are generally termed CFD. As opposed to CFD, MMM are fully equipped to include features such as cloud formation, precipitation and atmospheric radiative characteristics. Typical domain sizes are 50 – 2000 km, and typical spatial resolutions (grid cell sizes) are 1 – 100 km. MMM receive their boundary conditions from NWP or global meteorological models, or from MMM simulations at larger scales. Typically, non-resolved and sub-grid features such as surface-mounted obstacles (buildings, trees, etc.) are parameterized with approaches such as the main land-use approach, the parameter averaging method, the flux aggregation method and the canopy-layer approach [130]. An overview of MMM is given in [143]. As an example, Figure 7 displays results of the MM5 mesoscale model for the continental US, the southeastern US and the Appalachian region in a nested grid configuration with three domains at resolutions of 27 km, 9 km and 3 km [144]. Figures 7a-c show the ground temperature and wind vectors for domains 1, 2 and 3 at 16:01:12 GMT on Sept. 1, 1979, and Figures 7d-f show the topography and wind vectors for the same three domains and the same time.

In CFD, features such as cloud formation, precipitation and atmospheric radiative characteristics are generally not included. Instead, the transfer of heat and mass is resolved at much higher spatial and temporal resolution. Typical domain sizes range from 0.1 to 5 km, and typical spatial resolutions range from 0.1 m to 100 m. CFD can receive boundary conditions from MMM and/or from (semi-)empirical or theoretical

⁴ “Give me a lever long enough and a fulcrum on which to place it, and I shall move the world.”
Archimedes of Syracuse (c. 287 BC – c. 212 BC), Greek mathematician, physicist, engineer, inventor and astronomer.

expressions. Surface-mounted obstacles such as buildings and trees can be explicitly included in the computational domain. Whether they should be explicitly included or not, depends on their distance from the area of interest, as reported in the best practice guidelines mentioned in section 4.3. Generally, parameterization in CFD should be applied for obstacles smaller than the grid size. Examples are water ponds, sidewalks, benches, bushes, rocks, gravel, grass, etc. In addition, turbulence is parameterized to some extent, as explained above. As an example, Figure 8 shows two photographs and the corresponding view of a high-resolution computational grid of the campus of Eindhoven University of Technology [49]. Figure 8b shows that many buildings are explicitly included in the domain and grid (i.e. with their actual shape), while others – further away from the area of interest – are only included in a simplified way, and yet others are not included explicitly. The latter ones are included implicitly, by increased surface-roughness applied to the bottom of the computational domain. The same is done for trees, hedges and other features that constitute terrain roughness. This issue will be explained in more detail in section 5.2.

It should be noted that the spatial distance limits in Figure 6 are only indicative, particularly as related to model categories. Application of model categories outside these ranges is not uncommon. As computational resources have continued to increase over the past decades, also the boundaries between the model categories have continued to fade, where NWP / MMM are applied down to smaller scales and at higher grid resolutions, more explicitly resolving smaller terrain features (e.g. [143]). Similarly, CFD is applied at larger scales, with larger computational domains, with or without reductions in grid resolution. An example of a CFD study by the author with a very large computational domain is given in Figure 9, where CFD was employed to calculate the wind conditions in a narrow entrance channel in Galicia, Spain. The horizontal area of the domain is 25 x 20.5 km² and the minimum grid resolution is 2.5 m. In addition, several efforts have been made to couple MMM and CFD [130], to downscale MMM to include microscale meteorological effects [143] or to upscale CFD to include mesoscale meteorological influences [145], in an attempt to combine the strengths of both approaches and eliminate weaknesses.

Figure 6 also illustrates the three smaller scales in urban physics: the building scale, the building component scale and the scale of materials or humans. While these scales are generally not the focus in meteorology, they are of particular importance in urban physics. The building scale is key because the building is the place where people are born, work, live and die. The grand challenges climate, energy, health, security, aging cannot be properly addressed without incorporating the physical behavior of buildings. Indeed, many of the urban physics focus areas in Figure 4 and discussed in section 2 involve the building scale. Models applied at the building scale are CFD and Building Energy Simulation (BES). CFD is applied for both the indoor environment of buildings (e.g. review papers [70,146-148]), the outdoor environment of buildings (e.g. review papers [30,32,33,42-47,49-52,70]), and the combination of both, which is particularly evident in natural ventilation of buildings (e.g. review papers [67-77]). BES is applied for evaluating the energy performance of buildings, including energy consumption and thermal comfort [149-155]. CFD and BES are complementary. CFD is particularly suited for high-resolution modeling in space and time of velocity, temperature and concentration fields for statistically stationary conditions, i.e. for a fixed set of boundary conditions that represent a relatively short period in time (e.g. 10 minutes to an hour). Application of CFD to simulate long time periods (e.g. months to years), with changing boundary conditions, can become prohibitively expensive. BES on the other hand is particularly well suited for simulation of the energy behavior over such long time periods, at the expense of lower-resolution information on velocity, temperature and concentration in the building and building zones. As opposed to CFD, BES can easily and efficiently take into account a wide range of meteorological conditions that are relevant for building energy performance, such as solar radiation, long-wave radiation and cloudiness. It can also take into account solar shading, outdoor and indoor convective heat transfer, HVAC⁵ systems, internal gains by lighting and equipment, occupants, etc. Given their complementary character, efforts to couple and integrate of CFD and BES have been performed (e.g. [156,157]).

Also particularly relevant in urban physics is the building component scale, as building components – especially when they are characterized by open porosity – are the building parts that exchange heat and mass (air, moisture, pollutants, ...) with the indoor and outdoor air. The related model category is BC-HAM (Building Component – Heat, Air and Moisture transfer), also called BE-HAM (Building Envelope – HAM) (e.g. [158-164]). BC-HAM can easily and efficiently take into account a wide range of meteorological conditions that are relevant for building component performance, such as solar radiation, long-wave radiation and cloudiness. It can also take into account solar shading, outdoor and indoor convective heat transfer. Given its complementarity with CFD and with BES, coupling or combining BC-HAM and CFD has been performed (e.g. [165-167]), as well as coupling BC-HAM and BES (e.g. [168]).

At the scale of an individual person, Human Thermophysiology models are used, such as the IESD-Fiala model [169-171], the 65 MN model [172] and the Berkeley model [173], all of which are based on the Stolwijk

⁵ Heating, ventilation and airconditioning.

model [174,175]. Several efforts have combined CFD with HT models (e.g. [172-177]). Finally, at the material scale, Material Science Models (MSM) are employed, to study material behavior including adsorption and absorption characteristics and material degradation.

4. CFD for urban physics

First, a brief overview of the governing equations and their approximate forms is provided, as a prelude to an overview of best practice guidelines and to a discussion on RANS versus LES and to section 5, which is intentionally and mainly focused on RANS simulations. As opposed to section 3, section 4 focuses on urban physics in its narrower sense, i.e. CFD applied at the meteorological microscale and the building scale (outdoor environment).

4.1. Governing equations and approximate forms

The governing equations are the three laws of conservation: (1) conservation of mass (continuity); (2) conservation of momentum (Newton's second law); and (3) conservation of energy (first law of thermodynamics). While strictly the term Navier-Stokes (NS) equations only covers Newton's second law, in CFD it is generally used to refer to the entire set of conservation equations. The instantaneous three-dimensional NS equations for a confined, incompressible, viscous flow of a Newtonian fluid, in Cartesian co-ordinates and in partial differential equation form are:

$$\frac{\partial u_i}{\partial x_i} = 0 \quad (1a)$$

$$\frac{\partial u_i}{\partial t} + u_j \frac{\partial u_i}{\partial x_j} = -\frac{1}{\rho} \frac{\partial p}{\partial x_i} + \frac{\partial}{\partial x_j} (2\nu s_{ij}) \quad (1b)$$

$$\frac{\partial \theta}{\partial t} + u_j \frac{\partial \theta}{\partial x_j} = \frac{1}{\rho c_p} \frac{\partial}{\partial x_j} \left(k \frac{\partial \theta}{\partial x_j} \right) \quad (1c)$$

The vectors u_i and x_i are instantaneous velocity and position, p is the instantaneous pressure, θ the instantaneous temperature, t is time, ρ is the density, ν is the molecular kinematic viscosity, c_p the specific heat capacity, k the thermal conductivity and s_{ij} is the strain-rate tensor:

$$s_{ij} = \frac{1}{2} \left(\frac{\partial u_i}{\partial x_j} + \frac{\partial u_j}{\partial x_i} \right) \quad (1d)$$

In case of multi-component flow, an advection-diffusion equation for species concentration, similar to that for temperature, is added:

$$\frac{\partial c}{\partial t} + u_j \frac{\partial c}{\partial x_j} = \frac{\partial}{\partial x_j} \left(D \frac{\partial c}{\partial x_j} \right) \quad (1e)$$

where c is the instantaneous concentration and D the molecular diffusion coefficient or molecular diffusivity. Additional terms can be added to these equations, e.g. the gravitational acceleration term and the buoyancy term. As directly solving the NS equations for the high-Reynolds number flows in urban physics is currently prohibitively expensive, approximate forms of these equations are solved. Two main categories used in urban physics are RANS and LES. In addition, hybrid RANS/LES approaches are sometimes used.

The RANS equations are derived by averaging the NS equations (time-averaging if the flow is statistically steady or ensemble-averaging for time-dependent flows). With the RANS equations, only the mean flow is solved while all scales of the turbulence are modeled (i.e. approximated). The averaging process generates additional unknowns and as a result the RANS equations do not form a closed set. Therefore approximations have to be made to achieve closure. These approximations are called turbulence models. Up to now, RANS has been the

most commonly used approach in CFD in urban physics. Therefore, more detailed information about this approach is given below.

The RANS equations are obtained by decomposing the solution variables as they appear in the instantaneous NS equations (Eqs. 1a-c,e) into a mean (ensemble-averaged or time-averaged) and a fluctuation component. For an instantaneous vector \vec{a} and an instantaneous scalar ξ this means:

$$\vec{a} = \bar{\vec{A}} + \vec{a}' ; \quad \xi = \bar{\Xi} + \xi' \quad (2)$$

where $\bar{\vec{A}}$ and $\bar{\Xi}$ are the mean and \vec{a}' and ξ' the fluctuation components (around the mean). Replacing the instantaneous variables in Eq. (1a-c,e) by the sum of the mean and the fluctuation components and taking an ensemble-average or time-average of the resulting equations yields the RANS equations:

$$\frac{\partial U_i}{\partial x_i} = 0 \quad (3a)$$

$$\frac{\partial U_i}{\partial t} + U_j \frac{\partial U_i}{\partial x_j} = -\frac{1}{\rho} \frac{\partial P}{\partial x_i} + \frac{\partial}{\partial x_j} \left(2\nu S_{ij} - \overline{u_j' u_i'} \right) \quad (3b)$$

$$\frac{\partial \Theta}{\partial t} + U_j \frac{\partial \Theta}{\partial x_j} = \frac{1}{\rho c_p} \frac{\partial}{\partial x_j} \left(k \frac{\partial \Theta}{\partial x_j} - \overline{u_j' \theta'} \right) \quad (3c)$$

$$\frac{\partial C}{\partial t} + U_j \frac{\partial C}{\partial x_j} = \frac{\partial}{\partial x_j} \left(D \frac{\partial C}{\partial x_j} - \overline{u_j' c'} \right) \quad (3d)$$

Here, U_i , P , Θ and C are the mean velocity, pressure, temperature and concentration, u_i' , p' , θ' and c' are the fluctuation components and S_{ij} is the mean strain-rate tensor:

$$S_{ij} = \frac{1}{2} \left(\frac{\partial U_i}{\partial x_j} + \frac{\partial U_j}{\partial x_i} \right) \quad (4)$$

The horizontal bar in the equations denotes averaging. When comparing the set of equations (Eq. 1) with the instantaneous set (Eqs. 3-4), the similarity between both sets is observed, but also that the averaging process has introduced new terms, which are called the Reynolds stresses (for momentum), turbulent heat fluxes and turbulent mass fluxes. They represent the influence of turbulence on the mean flow, the heat transfer and the mass transfer. The instantaneous NS equations (Eq. 1a-c,e) form a closed set of equations (six equations with six unknowns: u_i , p , θ and c). The RANS equations do not form a closed set due to the presence of the Reynolds stresses and turbulent heat and mass fluxes (more unknowns than equations). It is impossible to derive a closed set of exact equations for the mean flow variables [178]. Closure must therefore be obtained by modeling. The modeling approximations for the Reynolds stresses are called turbulence models. Turbulence models are briefly discussed in section 4.2. Note that for including the effect of density differences due to temperature or species concentrations, generally the Boussinesq approximation for buoyancy is applied [179].

A distinction has to be made between steady RANS and unsteady RANS (URANS). Steady RANS refers to time-averaging of the NS equations and yields statistically steady descriptions of turbulent flow. However, flow in the atmospheric boundary layer (ABL) is inherently unsteady, and therefore, strictly, an unsteady approach is required. URANS refers to ensemble-averaging of the NS equations. Franke et al. [97] state that, since URANS also requires a high spatial resolution, it is recommended to directly use LES or hybrid URANS/LES. Regardless of spatial resolution, it is important to note that URANS does not simulate the turbulence, but only its statistics. In fact, URANS only resolves the unsteady mean-flow structures, while it models the turbulence. LES on the other hand actually resolves the large scales of the turbulence. URANS can be a good option when the unsteadiness is pronounced and deterministic, such as von Karman vortex shedding in the wake of an obstacle with a low-turbulence approach flow. However, given the relatively high turbulence in (approach-flow) atmospheric boundary layers, LES or hybrid URANS/LES should be preferred over URANS for these applications.

In the LES approach, the NS equations are filtered in space, which consists of removing only the small turbulent eddies (that are smaller than the size of a filter that is often taken as the mesh size). The large-scale

motions of the flow are solved, while the small-scale motions are modeled: the filtering process generates additional unknowns that must be modeled in order to obtain closure. This is done with a sub-filter turbulence model. LES generally shows superior performance compared to RANS and URANS, because a large part of the unsteady turbulent flow is actually resolved. However, the required computational resources increase significantly, the inlet boundary condition requires time and space resolved data and a larger amount of output data is generated.

The hybrid URANS/LES approach employs URANS in the near-wall region and LES in the rest of the domain. This approach is based on the fact that near walls, the turbulent eddies are very small and resolving them with LES could become prohibitively expensive. Note that this does not mean that stand-alone LES cannot yield good results for wall-bounded flows; in these situations often wall functions are used. A well-known hybrid approach is Detached Eddy Simulation [180], in which LES is combined with the one-equation Spalart-Allmaras turbulence model [181]. The application of hybrid approaches is not straightforward: URANS and LES are fundamentally different approaches with specific grid requirements which have to be matched where the switch between both occurs.

4.2. Turbulence modeling for RANS

As shown by a recent and detailed review of the literature in urban physics and wind engineering [51], steady RANS is by far most often used, in spite of its deficiencies. Studies that have employed unsteady RANS (URANS) are scarce. LES on the other hand is increasingly used, but by far not as often as steady RANS. Therefore, this section focuses on turbulence modeling for RANS.

Two main types of models can be distinguished: first-order closure and second-order closure models. First-order closure uses the Boussinesq eddy-viscosity hypothesis to relate the Reynolds stresses to the velocity gradients in the mean flow. Similarly, the turbulent heat fluxes are related to the mean temperature gradients and the turbulent mass fluxes to the mean concentration gradients. Second-order closure refers to establishing and solving additional transport equations for the Reynolds stresses and the turbulent heat and mass fluxes.

First-order closure is the simplest approach. The Boussinesq eddy-viscosity hypothesis calculates the Reynolds stresses as the product of a turbulent (eddy) viscosity and the mean strain-rate tensor:

$$-\overline{u_i' u_j'} = 2\nu_t S_{ij} - \frac{2}{3}k\delta_{ij} \quad (5)$$

where ν_t is the turbulent viscosity (also called momentum diffusivity), k is the turbulent kinetic energy and δ_{ij} is the Kronecker delta:

$$k = \frac{1}{2}\overline{u_i' u_i'} \quad (6)$$

$$\delta_{ij} = \begin{cases} 1 & \text{for } i = j \\ 0 & \text{for } i \neq j \end{cases} \quad (7)$$

In first-order closure, the turbulence models need to provide expressions for the turbulent (eddy) viscosity, and are called eddy-viscosity models. A distinction is made between linear and non-linear eddy-viscosity models. Examples are the one-equation Spalart-Allmaras model [181], the standard k - ϵ model [182] and its many modified versions, such as the Renormalization Group (RNG) k - ϵ model [183] and the realizable k - ϵ model [184], the standard k - ω model [185] and the k - ω shear stress transport (SST) model [186].

Similarly, the standard approximation for the turbulent flux of scalar quantities is the gradient-diffusion assumption, by which the turbulent heat and mass flux can be obtained as:

$$-\overline{u_j' \theta'} = D_{\theta,t} \frac{\partial \Theta}{\partial x_j} \quad (8)$$

$$-\overline{u_j' c'} = D_{c,t} \frac{\partial C}{\partial x_j} \quad (9)$$

where $D_{\theta,t}$ and $D_{c,t}$ are the turbulent heat and mass diffusivities, which are generally related to the momentum

diffusivity by the turbulent Prandtl number Pr_t and the turbulent Schmidt number Sc_t , respectively:

$$Pr_t = \frac{\nu_t}{D_{\theta,t}} \quad (10)$$

$$Sc_t = \frac{\nu_t}{D_{c,t}} \quad (11)$$

Neither $D_{\theta,t}$ nor $D_{c,t}$ is a fluid property. Instead, like the turbulent viscosity ν_t , they are a function of the type of flow pattern and the location in this flow pattern. The same holds for Pr_t and Sc_t . Nevertheless, often constant values are used for Pr_t and Sc_t in RANS CFD simulations. This constitutes an important simplification and can give rise to serious errors.

Second-order closure is also referred to as second-moment closure or Reynolds Stress modeling (RSM). It consists of establishing and solving additional transport equations for each of the Reynolds stresses and the turbulence dissipation rate. Second-order closure is also possible for the turbulent heat and mass fluxes, but this option is not often used in CFD in urban physics.

4.3. CFD best practice guidelines ⁶

In CFD simulations, a large number of choices need to be made by the user. It is well known that these choices can have a very large impact on the results. Already since the start of the application of CFD for wind flow around bluff bodies in the late 70s and 80s, researchers have been testing the influence of these parameters on the results, which has provided a lot of valuable information (e.g. [187-191]). In addition, Schatzmann et al. [192] provided an important contribution on validation with field and laboratory data. However, initially this information was dispersed over a large number of individual publications in different journals, conference proceedings and reports.

In 2000, the ERCOFTAC⁷ Special Interest Group on Quality and Trust in Industrial CFD published an extensive set of best practice guidelines for industrial CFD users [193]. These guidelines were focused on RANS simulations. Although they were not specifically intended for urban physics, many of these guidelines also apply for urban physics. Within the EC project ECORA⁸, Menter et al. [194] published best practice guidelines based on the ERCOFTAC guidelines but modified and extended specifically for CFD code validation. Within QNET-CFD⁹, the Thematic Area on Civil Construction and HVAC (Heating, Ventilating and Air-Conditioning) and the Thematic Area on the Environment presented some best practice advice for CFD simulations of wind flow and dispersion [195,196].

In 2004, Franke et al. [96] compiled a set of specific recommendations for the use of CFD in wind engineering from a detailed review of the literature, as part of the European COST¹⁰ Action C14: Impact of Wind and Storm on City Life and Built Environment. Later, this contribution was extended into an extensive “*Best Practice Guideline for the CFD simulation of flows in the urban environment*” [97,102], in the framework of the COST Action 732: Quality Assurance and Improvement of Microscale Meteorological Models, managed by Schatzmann and Britter (<http://www.mi.uni-hamburg.de/Home.484.0.html>). Like the ERCOFTAC guidelines, also these guidelines primarily focused on steady RANS simulations, although also some limited information on URANS, LES and hybrid URANS/LES was provided. When using CFD tools, whether they are academic/open source or commercial codes, it is also important that the code is well documented, and that basic verification tests and validation studies have been successfully performed and reported. A good description of how a microscale airflow and dispersion model has to be documented can be found in the Model Evaluation Guidance Document published in the COST Action 732 by Britter and Schatzmann [197].

In Japan, working groups of the Architectural Institute of Japan (AIJ) conducted extensive cross-comparisons between CFD simulation results and high-quality wind-tunnel measurements to support the development of guidelines for practical CFD applications. Part of these efforts were reported by Yoshie et al. [48]. In 2008, Tominaga et al. [98] published the “*AIJ guidelines for practical applications of CFD to*

⁶ This section is intentionally reproduced from ref. [51] (Blocken (2014) in Journal of Wind Engineering & Industrial Aerodynamics), for completeness of the present paper and because of its importance to sections 4.4 and 5 of the present paper.

⁷ ERCOFTAC = European Research Community on Flow, Turbulence and Combustion

⁸ ECORA = Evaluation of Computational Fluid Dynamic Methods for Reactor Safety Analysis

⁹ QNET-CFD = Network for Quality and Trust in the Industrial Application of CFD

¹⁰ COST = European Cooperation in Science and Technology

pedestrian wind environment around buildings”, and Tamura et al. [100] wrote the “*AIJ guide for numerical prediction of wind loads on buildings*”. The guidelines by Tominaga et al. [98] focus on steady RANS simulations, while the guidelines by Tamura et al. [100] also consider LES, given the importance of time-dependent analysis for wind loading of buildings and structures.

More generic best practice advice was provided by Jakeman et al. [198] in the article “*Ten iterative steps in development and evaluation of environmental models*”, which were later on extended to development and evaluation of process-based biogeochemical models of estuaries by Robson et al. [199] but also to CFD for environmental fluid mechanics (including urban physics) by Blocken and Gualtieri [128]. Blocken et al. [49] also provided a general decision framework for the analysis of pedestrian-level comfort and safety in urban areas.

These best practice guideline documents have been based on and/or reinforced by more basic guidelines and standards concerning verification and validation, e.g. those developed by Roache [200,201], AIAA¹¹ [202], Oberkampf et al. [203], Roy [204], Roy and Oberkampf [205], ASME¹² [206], and others. It is interesting to note that the importance of numerical accuracy control is emphasized by the Journal of Fluids Engineering Editorial Policy [207], incited by contributions by Roache et al. [208] and Freitas [209], which demand at least formally second-order accurate spatial discretisation.

In addition to these general guidelines, also some very specific guidelines were published. These include (1) consistent modeling of equilibrium atmospheric boundary layers in computational domains (e.g. [97,210-218]); (2) high-quality grid generation (e.g. [219,220]) and (3) validation with field and laboratory data (e.g. [192,221]). Note that most of the efforts in the first two areas were focused on steady RANS simulations.

The establishment of these guidelines has been an important step towards more accurate and reliable CFD simulations.

4.4. RANS versus LES: possibilities and limitations

LES is intrinsically superior in terms of physical modeling to both RANS and URANS. It is widely recognized that its theory is well developed and that it is very suitable for simulating the three specific characteristics of turbulent bluff body flow in urban physics: three-dimensionality of the flow, unsteadiness of the large-scale flow structures and anisotropy of turbulent scalar fluxes [43]. In addition, its application is increasingly supported by ever increasing computing resources. However, for most focus areas in urban physics (Fig. 4), 3D steady RANS remains the main CFD approach up to the present day. In many of these focus areas and in many practical studies, it is often being applied with a satisfactory degree of success (e.g. [31,33,42,48,49,51,73,77,123,212,220-236]). A detailed review of the literature [51] shows that this statement seems to hold for the focus areas thermal environment, pedestrian-level wind, natural ventilation, wind-driven rain, snow transport, vehicle aerodynamics and wind energy. Also for topics such as pollutant dispersion, where LES can offer much higher accuracy than steady RANS, many researchers and practitioners keep using the latter approach [43-45].

To the opinion of the present author, two main reasons are responsible for the continued use of 3D steady RANS. First, as expected, the computational cost of LES. This cost is at least an order of magnitude larger than for steady RANS, and possibly two orders of magnitude larger when including the necessary actions for verification and validation. Second: the lack of quality assessment in practical applications of LES, the lack of best practice guidelines in LES and therefore the lack of confidence in LES. These arguments are further explained below.

Even without the necessary actions for verification and validation, LES remains very computationally demanding, and often too computationally demanding for practical applications, where generally simulations need to be made for at least 12 wind directions [48], and sometimes even more. When the necessary actions of quality assurance are included – as they should – simulations for several of these different wind directions should be performed on different grids and with different subgrid-scale models to ensure the accuracy and reliability of the simulations. This can be done using techniques such as the Systematic Grid and Model Variation technique (e.g. [237-239]). These techniques are well developed and very valuable, but they are very rarely applied in urban physics LES simulations. However, care for accuracy and reliability is especially important in LES because, as stated by Hanna [240]:

“... as the model formulation increases in complexity, the likelihood of degrading the model’s performance due to input data and model parameter uncertainty increases as well.”

¹¹ AIAA = American Institute of Aeronautics and Astronautics

¹² ASME = American Society of Mechanical Engineers

This motivates the establishment of generally accepted and extensive best practice guideline documents for LES in urban physics. However, while several sets of such guidelines have been developed for RANS in the past 15 years, as outlined in section 4.3, this is not to the same extent the case for LES. This in turn is caused by the computational expense of LES, as the establishment of such guidelines requires extensive sensitivity testing.

The above statements are confirmed by the extensive blind comparison test of microscale flow models (including RANS and LES) reported by Bechmann et al. in 2011 [241] for wind flow over the small Bolund hill, a topographic feature in Denmark. Based on this comparison, they state that:

“... the wind industry will in any case be reluctant to switch to more sophisticated methods if they have not been verified and validated. Until then, the use of LES for terrain flows will mostly be limited to single-case studies and not used as a standard tool. Solution of the RANS equations with a two-equation closure is more computationally economical, gives good results and has matured from the stage of research tool to a level whereby it can be implemented in the wind industry”.

It is argued that this statement holds equally well for LES versus RANS in urban physics. In this perspective, Yoshie et al. in 2007 [48] stated:

“However, in order to use LES in general-purpose applications for predicting the wind environment around buildings, we need a dramatic increase in computer processing speed in the future. For the time being, we must be content with RANS type models currently in use.”

Two other relevant quotes were provided by Hanjalic in 2004 [124] and Baker in 2007 [123]:

“It is argued that RANS will further play an important role, especially in industrial and environmental computations, and that the further increase in the computing power will be used more to utilize advanced RANS models to shorten the design and marketing cycle rather than to yield the way to LES.” [124]

“The CFD techniques that will prove to be of most use will be those that will faithfully model the turbulence structure within the atmospheric boundary layer, e.g. LES or DES techniques. The use of RANS based techniques will decrease over time, although their relative simplicity and economy will ensure their continued use for many applications.” [123]

While these statements were made quite some years ago, they still equally apply today.

5. Ten tips and tricks towards accurate and reliable CFD simulations

*“Assiduus usus uni rei deditus et ingenium et artem saepe vincit”*¹³

This section provides ten tips and tricks towards accurate and reliable CFD simulations in urban physics, with focus on the meteorological microscale and the building scale (outdoor environment). These tips and tricks are certainly not intended to be complete, rather they are intended to complement the existing and very valuable CFD best practice guidelines for urban physics on ten particular aspects. The most extensive best practice guidelines for urban physics are those by Franke et al. [96,97] and Tominaga et al. [98]. As these and most other CFD best practice guidelines, also the tips and tricks in this section are mainly directed to RANS simulations.

5.1. Create a computational domain based on the directional blockage ratio

In general, only the bottom of the computational domain corresponds to an actual physical boundary. The side and top faces of the computational domain are non-physical boundaries, and they should be located far enough from the urban or building model to avoid too strong artificial acceleration of the flow due to too strong contraction of the flow by these boundaries (Fig. 10a,b; Venturi-effect: [242]). Based on sensitivity

¹³ “Constant practice devoted to one subject often outdoes both intelligence and skill”. Marcus Tullius Cicero (106 BC – 43 BC), Roman philosopher, politician, lawyer, orator, political theorist, consul and constitutionalist.

tests, three types of specific guidelines have been established to determine the size of the computational domain: Type-1: guidelines that impose minimum distances between the urban or building model and the boundaries of the domain; Type-2: guidelines that impose a maximum allowed blockage ratio; and Type-3: guidelines that are a combination of Types 1 and 2. The blockage ratio is defined as in wind-tunnel testing [243,244]: it is the ratio of the projected frontal (windward) area of the obstacles to the cross-section of the computational domain (Fig. 10d), and in CFD it is generally required to be less than 3%:

$$BR = \frac{A_{\text{building}}}{A_{\text{domain}}} \leq 3\% \quad (12)$$

The guidelines by Franke et al. [96,97] are Type-3 guidelines, based on those by Baetke et al. [189] and Hall [191]. They are represented in Figure 10c,d. The inlet, lateral and top boundary should be at least $5H_{\text{max}}$ away from the group of explicitly modeled buildings, where H_{max} is the height of the tallest building. The outflow boundary should be at least $15H_{\text{max}}$ away from the group of explicitly modeled buildings, to allow for full wake flow development. The blockage ratio should not be larger than 3%. Note that this guideline is more stringent than the 5% limit imposed in wind-tunnel testing [243,244].

The guidelines by Tominaga et al. [98] also impose a maximum blockage ratio of 3%. They demand the lateral and top boundary of the domain to be at least $5H_{\text{max}}$ away, the distance between the inlet boundary and the model to be equal to the upwind area covered by a smooth floor in a corresponding wind-tunnel test, and the outflow boundary to be at least $10H_{\text{max}}$ downstream.

Although these guidelines are often necessary and will also be sufficient for many studies, they are not necessarily sufficient to avoid unwanted artificial acceleration in some exceptional but not uncommon cases. In particular for buildings that are very wide or for urban models - that are typically very extended in the horizontal direction - it is possible that, although the above-mentioned guidelines are satisfied (Eq. (12) and all minimum distances), still an unacceptable degree of artificial acceleration will occur on the sides of the building or urban model. This can be easily seen in Figure 10e, where the cross-section of the computational domain for the wide building satisfies all above-mentioned guidelines, but clearly artificial acceleration will occur at the sides of the building because the lateral sides of the domain are too close to the building model. To avoid this unwanted situation, the present paper suggests the concept of the directional blockage ratio. This new concept consists of the decomposition of both the blockage ratio and the 3% limit in the horizontal and vertical lateral direction, where the limit for each is the square root of 3%, i.e. about 17%:

$$BR_L = \frac{L_{\text{building}}}{L_{\text{domain}}} \leq 17\% \quad (13)$$

$$BR_H = \frac{H_{\text{building}}}{H_{\text{domain}}} \leq 17\% \quad (14)$$

These demands are more stringent than Eq. (12) but their satisfaction automatically leads to satisfaction of Eq. (12). They should be applied together with the Type-1 requirements. The resulting cross-section of the computational domain is illustrated in Figure 10f.

5.2. Create a high-quality computational grid consisting only of prismatic cells

The computational grid is the Achilles heel of many CFD simulations in urban physics. Because of the generally rather complex model geometry, also the computational grid is often quite complex. In far too many CFD simulations, insufficient time is spent to generate a high-quality grid, leading to inferior results or to convergence problems, or both. Indeed, high-quality computational grids are not only important to reduce the discretization error but also to allow convergence of the iterative process with the minimum required second-order discretization schemes. Researchers that submit papers to international journals often report that they had to use of first-order discretization schemes “*because the simulation would not converge with higher-order schemes*”. This practice actually corresponds to compensating poor grid quality with numerical diffusion errors caused by the use of first-order schemes. This numerical or artificial diffusion indeed has a stabilizing effect on the convergence process, exactly because it introduces errors. Clearly, this practice should be abandoned, and, as recommended by best practice guidelines, always high-quality grids and higher-order discretization schemes should be used (see also section 5.5).

Two characteristics of high-quality computational grids are (i) sufficient overall grid resolution and (ii) quality of the computational cells in terms of shape (including skewness), orientation and stretching ratio. The existing best practice guidelines provide important advice on both aspects. In terms of overall grid resolution, Franke et al. [96] state that the grid should be fine enough to capture the important physical phenomena like shear layers and vortical structures with sufficient resolution. For urban and building models, they advise to use at least 10 cells per cube root of the building volume, and 10 cells in between every two buildings. For studies of pedestrian-level wind speed, the focus height of 1.5 – 2 m should coincide with the 3rd of 4th cell above ground level. Finally, the overall resolution needs to be analyzed by a grid-convergence study, for which at least three systematically and substantially refined grids should be used, with a refinement factor of at least 3.4 (combination of all three coordinate directions). This study should be accompanied by error assessment by generalized Richardson extrapolation. In terms of the quality of computational cells, they advise to keep the stretching ratio below 1.3 in regions of high gradients, to limit the truncation error. They also advise the use of hexahedral cells over tetrahedral cells, as hexahedra yield smaller truncation errors and better iterative convergence. In addition, on walls, the grid lines should be perpendicular to the wall [193,194], which implies that tetrahedral cells should not be used *at* the walls.

In terms of overall grid resolution, Tominaga et al. [98] advise a grid-convergence study until the prediction result does not change significantly anymore with increasing grid resolution. The linear refinement factor (in each coordinate direction) should be at least 1.5, based on [246], which yields $1.5^3 = 3.375$, almost the same as the 3.4 from [96]. Concerning the quality of computational cells, Tominaga et al. [98] advise that the grid should especially capture the characteristics of the separating flows on roof and walls. They also mention that for bluff bodies with sharp edges, the use of wall functions generally does not entail significant loss of accuracy, because for such bodies the separation points are always at the sharp leading edges. They advise a minimum of 10 grid cells on every side of a building to correctly reproduce the separated flow. Stretching ratios in regions of high velocity gradients should be 1.3 or less. The evaluation height (1.5 – 5.0 m above ground) should be located at the 3rd or more grid cell from the ground. Finally, for unstructured grids, they recommend to arrange the boundary layer cells, which should be prismatic cells, parallel to the walls or the ground surfaces. This important advice is graphically depicted in Fig. 11.

Van Hooff and Blocken [220] presented a relatively easy-to-use grid-generation technique that allows to satisfy all of the above guidelines even for very complex building and urban geometries. They called this technique the *surface-grid extrusion technique*. It allows to efficiently and simultaneously generate the geometry and the computational grid. It is a body-fitted technique that consists of a series of extrusion operations, i.e. it creates the geometry and the grid based on geometrical translation and rotation operations of pre-meshed 2D cross-sections. This way, it allows full control over grid quality and grid resolution, contrary to standard semi-automatic unstructured grid generation procedures that, especially for complex building geometries, often lead to unstructured grids of low quality. The technique only uses prismatic cells. It also provides a way to easily implement various changes in the model geometry and grid for parametric studies. The procedure was first applied for the rather complex Amsterdam ArenA football stadium in the Netherlands [220,247,248]. The computational geometry of the stadium and its surroundings and the resulting high-quality computational grid are illustrated in Figure 12. The grid-generation technique that led to the grid in Figure 12b is briefly outlined below and schematically depicted in Figure 13a. It consists of the following steps:

1. Creating the geometry and the grid of the vertical stadium cross-section (indicated by “1” in Fig. 13a). Both the solid and fluid parts of this cross-section are meshed;
2. Defining a line A in the ground plane which represents the inner stadium circumference, and applying a grid to this line;
3. Extruding cross-section “1” (geometry and grid) along line A. This way, both the geometry and the volume grid of the stadium circumference are generated. The volume grid is generated based on the cross-section grid and the grid on line A. Note that at this stage, both solid and fluid volumes are meshed;
4. Applying a grid to the bounded plane “2”, which is that part of the ground plane of which line 1 represents the circumference; this plane represents the stadium interior;
5. Extruding plane “2” (geometry and grid) vertically along line B. This way, both the geometry and the volume grid of the stadium interior are generated, up to the end position of line B;
6. Defining all lines in the ground plane outside the stadium that represent the circumference of the surrounding buildings, streets and squares. The outermost lines are the bounds of the bottom of the computational domain;
7. Applying a surface grid to the collection of planes “3” that are bounded by these lines;
8. Extruding all planes “3” (geometry and grid) vertically along line C;
9. Defining a line D which starts at the top of the stadium cross-section, defined in step 1, and ends at the roof height of the lowest building that is higher than the end point of line B. Defining a line E

which starts at the end point of line D, and ends at the roof height of the lowest building that is higher than the end point of line D, and so on for lines F, G, etc., up to the intended height of the computational domain;

10. Extruding all horizontal planes (geometry and grid) at the height of the starting point of line D vertically along line D, next along line E, and so on. The final extrusion also generates the top surface of the domain. The result is a rectangular prism (the computational domain) that is completely meshed and that contains all buildings;
11. Deleting the grid at the location of the intended solid domain parts (buildings and building parts). This way, solid volumes are introduced and only the fluid domain remains meshed.

Figure 13b illustrates the application of this procedure for the actual stadium geometry by showing a few cross-sections and part of the generated volume grids. The advantages of this systematic procedure are:

- Simultaneous generation of geometry and grid for both the outdoor and indoor environment (see Fig. 14 for the case of the Amsterdam ArenA stadium);
- Full control over grid generation yielding a body-fitted grid without tetrahedral cells;
- The possibility to satisfy the guidelines by Franke et al. [96,97] and Tominaga et al. [98];
- Reduced convergence problems with higher-order discretization schemes when compared to lower-quality unstructured grids;
- The possibility to a priori implement different geometrical variations in the model/grid, as outlined in [220,247].

In later publications, the power of this technique has been illustrated by application to a range of simple to complex building and urban configurations [19,41,49,73,77,229-232,234,235,247-255], some of which are illustrated in Figure 8, 9 and 15.

5.3. Determine and impose the appropriate roughness parameters

Accurate simulation of ABL flow in the computational domain is imperative for accurate and reliable simulation of the related urban physics processes [210-218]. Correct specification of appropriate roughness parameters is an essential component of accurate simulation of the ABL.

First, a distinction is made between five spatial areas in which roughness should be specified (Fig. 16):

1. Area 1: The area upstream of the computational domain. This roughness should be carefully estimated because it should be used to determine the shape of the inlet profiles of mean wind speed and turbulence quantities that are applied at the inlet plane of the computational domain. This roughness is a large-scale roughness, termed aerodynamic roughness length $z_{0,1}$. It can be estimated based on land-use maps in combination with the roughness classification by Davenport¹⁴, updated by Wieringa [256] (Table 1 in this article). This estimate should typically be conducted for an upstream fetch of 5-10 km, as this is the typical distance needed for the ABL to adjust to the underlying terrain roughness. Estimating $z_{0,1}$ from Table 1 is not straightforward, as the description is qualitative and the terrain roughness is generally heterogeneous over the 5-10 km fetch. As a result, it is easy to be at least one class off in Table 1, and this uncertainty should be taken into account in the interpretation of the results. An example of estimating $z_{0,1}$ for terrain upstream of a computational domain is given in Figure 9a, where estimates are provided for 12 different wind direction sectors.
2. Area 2: The area inside the computational domain and upstream of the explicitly modeled buildings (Fig. 16). Often, this is an area where buildings or other obstacles are present, but because these do not belong to the area of interest, they are not modeled explicitly (i.e. not with their actual main shape), but only implicitly. This allows saving computational resources (grid cells). The aerodynamic roughness length $z_{0,2}$ of this area should be estimated again using the Davenport-Wieringa roughness classification [256].
3. Area 3: The area inside the computational domain representing the ground surface amidst the explicitly modeled buildings and other obstacles. This area typically contains small-scale topographic features that are not modeled explicitly, such as sidewalks, benches, fences, trees, hedges, etc. These should be implicitly modeled. Two approaches can be used. The first is to implement them as an increased surface roughness $z_{0,3}$. Again, this value can be estimated from the Davenport-Wieringa roughness classification [256], although this is not straightforward. The

¹⁴ Alan Garnett Davenport (1932-2009), one of the founding fathers of the discipline of wind engineering and founder of the Boundary Layer Wind Tunnel Laboratory (BLWT) at the University of Western Ontario, London, Canada.

second is to implement them as source and sink terms in the governing equations and the equations of the turbulence model. Some examples of implicit modeling of vegetative features can be found in [253-255,257-261].

4. Area 4: The surfaces of the explicitly modeled buildings (facades, roofs) and structures inside the computational domain. Buildings and other structures such as bridges have rough surfaces, the roughness of which can be characterized by an equivalent sand-grain roughness height $k_{s,4}$.
5. Area 5: The area inside the computational domain and downstream of the explicitly modeled buildings (Fig. 16). This area is generally less important, as it is situated downstream of the area of interest and the upstream aerodynamic disturbance of downstream terrain features is rather limited. The aerodynamic roughness length $z_{0,5}$ of this area can be estimated again using the Davenport-Wieringa roughness classification [256].

Second, a distinction is made between the two types of roughness specification [211,212]:

1. aerodynamic roughness length z_0 ;
2. equivalent sand-grain roughness height k_s .

In urban physics CFD simulations, both are sometimes incorrectly exchanged, which can lead to very large simulation errors [212] because typically, k_s is at least one order of magnitude larger than z_0 . The confusion can be caused by the fact that some CFD codes use wall functions with roughness modification based on z_0 , while others use wall functions with roughness modification based on k_s . The concept of aerodynamic roughness length z_0 is typically associated with large-scale terrain roughness (Table 1, [256]). The concept of equivalent sand-grain roughness length k_s on the other hand typically refers to small-scale surface roughness. It is due to Nikuradse¹⁵ [262] who investigated flow in roughened pipes and channels where the roughness was applied by sand-grains. Because many CFD codes were initially developed for mechanical engineering applications and flow in machinery in which the small-scale roughness is relevant, many of the wall functions in these codes include roughness modifications based on k_s . A well-known example are the standard wall functions by Launder and Spalding [263] and their roughness modification by Cebeci and Bradshaw [264], which were and still are present in the commercial CFD codes ANSYS/Fluent, CFX and in the non-commercial CFD code OpenFOAM.

While these wall functions and this roughness modification are very suitable for small-scale roughness, they should be used with care for large-scale roughness. At far too many occasions, these wall functions have been used for urban physics applications, and the value of z_0 has incorrectly been used as input value instead of the value for k_s [211,212]. In 2007, Blocken et al. [211] first derived the exact relationship between z_0 and k_s for several codes based on first-order matching between ABL velocity profiles and wall functions, yielding, for ANSYS/Fluent and OpenFOAM:

$$k_{s,ABL} = \frac{9.793 z_0}{C_s} \quad (15)$$

Where C_s is the roughness constant. For ANSYS-CFX, the relationship is:

$$k_{s,ABL} = 29.6 z_0 \quad (16)$$

The approach of first-order matching in [211] can be applied to every CFD code and every wall function, to yield the required relationship between z_0 and k_s .

In conclusion, the advice is as follows. First, assess carefully which wall functions and which roughness modification are present in the CFD code. Next:

1. If the CFD code is equipped with both wall functions based on z_0 and wall functions based on k_s , the former should be used for areas 1, 2, 3 and 5, while the latter should be used for area 4.
2. If the CFD code is only equipped with wall functions based on z_0 , its application for areas 1, 2, 3 and 5 is straightforward. For area 4, first a reasonable estimate of the small-scale roughness $k_{s,4}$ should be made, after which it should be converted to the equivalent value for $z_{0,4}$ using equations such as Eq. (15) and (16), and this value should be inserted into the wall function.
3. If the CFD code is only equipped with wall functions based on k_s , the application for area 4 is straightforward. For areas 1, 2, 3 and 5, first a reasonable estimate of the large-scale roughness $z_{0,1}$, $z_{0,2}$, $z_{0,3}$ and $z_{0,5}$, should be made, after which these values should be converted to the equivalent values for $k_{s,1}$, $k_{s,2}$, $k_{s,3}$ and $k_{s,5}$ using equations such as Eq. (15) and (16), and these values should be inserted into the wall function. It should be noted that especially the values of $k_{s,1}$, $k_{s,2}$ and $k_{s,5}$ will be very large. Indeed, it is important to realize that these values of equivalent sand-grain roughness

¹⁵ Johann Nikuradse (1894-1979), Georgia-born German engineer and physicist.

height should exert the same effect on the flow as the corresponding values of $z_{0,1}$, $z_{0,2}$ and $z_{0,5}$, a situation that is schematically depicted in Figure 17.

5.4. Set appropriate inlet boundary conditions

Setting appropriate inlet boundary conditions has a dual component: (i) using an appropriate estimate of the upstream aerodynamic roughness length, as outlined in section 5.3; (ii) using appropriate basic expressions of the vertical profiles for mean velocity and turbulence properties. As outlined in section 3, CFD can receive boundary conditions from MMM and/or from (semi-)empirical or theoretical expressions. The most often used profiles for RANS CFD simulations in urban physics and wind engineering are those presented by Richards and Hoxey in their pioneering 1993 paper on “*Appropriate boundary conditions for computational wind engineering models using the k-ε turbulence model*” [210]:

$$U(z) = \frac{u_{ABL}^*}{\kappa} \ln \left(\frac{z + z_0}{z_0} \right) \quad (17)$$

$$k(z) = \frac{u_{ABL}^{*2}}{\sqrt{C_\mu}} \quad (18)$$

$$\varepsilon(z) = \frac{u_{ABL}^{*3}}{\kappa (z + z_0)} \quad (19)$$

where u_{ABL}^* is the ABL friction velocity, κ the von Karman constant (0.42) and C_μ a constant, generally taken equal to 0.09. When using specific values for the turbulence model constants (see [210]), these expressions are an analytical solution to the RANS equations and the two equations of the standard k-ε model. As such, it represents an elegant set of inlet conditions. Later, Richards and Norris [218] extended this work by also providing boundary conditions for other RANS turbulence models. However, field measurements and reduced-scale wind-tunnel measurements of turbulence intensity do not always yield a profile of turbulent kinetic energy k that is constant with height in the surface layer, as suggested by Eq. (18).

Tominaga et al. [98] provide an alternative by specifying that $k(z)$ can be obtained from a wind-tunnel experiment or an observation of corresponding surroundings. If these are not available, they suggest a specific profile for the streamwise turbulence intensity $I_u(z)$:

$$I_u(z) = \frac{\sigma_u(z)}{U(z)} = 0.1 \left(\frac{z}{z_G} \right)^{(-\alpha-0.05)} \quad (20)$$

where z_G is the ABL height related to the terrain aerodynamic roughness length and α is the power-law exponent [98]. The turbulent kinetic energy can then be estimated from:

$$k(z) = \frac{\sigma_u^2(z) + \sigma_v^2(z) + \sigma_w^2(z)}{2} \cong \sigma_u^2(z) = (I_u(z) U(z))^2 \quad (21)$$

The above Eqs. (17-21) constitute important guidelines. As a minor supplement to the above, it is noted that the assumption in Eq. (21) is supported by the fact that in the lowest level of the ABL, the surface layer, the standard deviations of the turbulent fluctuations are approximately constant in the case of strong winds. Typical values of σ_u , σ_v and σ_w were obtained from observations at various locations with uniform terrain. Those values, as reported by Panofsky and Dutton [265], are $\sigma_u = 2.4 u^*$, $\sigma_v = 1.9 u^*$ and $\sigma_w = 1.25 u^*$. This yields: $\sigma_u^2 = 1.11(\sigma_v^2 + \sigma_w^2)$. Therefore, it can indeed reasonably be taken that $\sigma_u^2 \approx \sigma_v^2 + \sigma_w^2$, and Eq. (21) is good advice.

Note however that the above-mentioned profiles assume an ABL that has developed over a fetch of uniform roughness of at least 5 km. In practical urban physics simulations, the fetch will generally be heterogeneous, which substantially complicates things. Special care is then required in interpretation of the results. The above-mentioned profiles also assume a neutrally-stratified ABL. The profiles for stably and unstably stratified conditions can be considerably different.

5.5. Select higher-order discretization schemes

First-order discretization schemes should never be used because of their known problems in terms of numerical diffusion. This statement is corroborated by Tominaga et al. [98] and Franke et al. [96,97]. As mentioned earlier, the importance of numerical accuracy control is emphasized by the Journal of Fluids Engineering Editorial Policy [207], incited by contributions by Roache *et al.* [208] and Freitas [209], which demand at least formally second-order accurate spatial discretisation. As mentioned in section 5.2, the use of first-order schemes is often proof of inadequate grid quality. When a high-quality grid is generated, which – although rather time-consuming – is possible even for very complex building and urban geometries, e.g. using the surface-grid extrusion technique outlined in section 5.2, the use of second-order schemes should be perfectly possible without compromising convergence behavior.

5.6. Set stringent iterative convergence criteria and beware of oscillatory convergence

Many CFD codes use convergence criteria that are (much) too lenient, such as a termination threshold of 0.001 for the scaled residuals. Certainly for complex flow problems as encountered in urban physics, this will generally not be sufficient to get a converged solution. Typical problem areas where convergence is delayed are passages between buildings and other areas of high wind speed gradients. Franke et al. [97] indeed correctly mention that 0.001 is generally too high to have a converged solution, and that a reduction of at least four orders of magnitude is recommended. Tominaga et al. [98] also state that default values in CFD codes are often not strict enough. They impose more stringent requirements by demanding monitoring of variables at specific points or by overlapping contours of calculations results at different time steps.

In addition to these valuable guidelines, the present paper warns for oscillatory convergence in steady RANS simulations. When flow problems that are inherently transient are forced into a steady simulation, and when numerical diffusion is limited, it is possible that oscillatory convergence occurs. This implies that not a single converged solution is obtained, but that the solution depends on the number of preceding iterations [73]. This is not an indication of a lower-quality simulation. On the contrary, it indicates that the grid resolution is high enough and numerical diffusion is low enough for non-linear effects to influence the convergence process. A detailed comparison by Ramponi and Blocken [73] of such CFD results with the high-quality Particle Image Velocimetry (PIV) measurements by Karava et al. [266] indicated that accurate results could only be obtained by averaging the CFD results over at least a period of oscillatory behavior. In addition, these simulations showed that the results at different numbers of preceding iterations corresponded to modes of the actual transient behavior of the natural ventilation flow, with a flapping jet entering the building and with signs of vortex shedding in the wake. Figure 18 illustrates some results of this study. Figure 18c-e show the oscillatory behavior of the converged solution, where oscillations are found for all residuals (Fig. 18d) but not for all points in the flow field (Fig. 18e). Note that points 2 and 3, which show oscillatory convergence, belong to the regions in the actual flow field that are characterized by unsteadiness (flapping of jet in pt. 2 and vortex shedding in pt. 3).

The advice is to first allow convergence to continue until residuals do not change any more or enter into oscillatory convergence. In the latter case, the iterative process should be continued and solutions at different stages in this second stage of the iterative process should be stored and averaged to yield the final averaged solution.

5.7. Test horizontal (in)homogeneity in an empty computational domain

This refers to two separate aspects: (i) Checking whether the correct type of roughness has been used for the inlet profiles ($z_{0,1}$) and for the upstream part of the computational domain ($z_{0,2}$; $k_{s,2}$; $C_{s,2}$). Typically, $z_{0,1}$ and $z_{0,2}$ are taken the same, as they are often assessed together from the roughness classification; (ii) Checking whether the inlet profiles and the incident profiles are not too different. As depicted in Figure 16, the incident profiles are those actually impinging on the urban or building model. As this model also exerts an upstream disturbance on the approach-flow profiles, the incident profiles should be determined from a simulation in an empty domain. The incident profiles are important because these are the profiles to which the model is actually subjected. For the empty domain simulation, the inlet profiles and roughness specifications should be the same as in the actual simulation with the building models present.

In wind-tunnel modeling, generally only either the approach-flow profiles (i.e. at some position upstream of the urban or building mode) or the incident profiles are measured. It is very important that the wind-tunnel report indicates which profiles were measured – often this is not done. This can compromise the value of the wind-tunnel measurement results for CFD validation.

5.8. Perform a grid convergence analysis and report it with the grid convergence index

Section 5.2 mentioned the importance of high-quality grid generation. The surface-grid extrusion technique in section 5.2 should be repeated at least three times, yielding three computational grids for a grid convergence analysis. The difference in total number of cells between every two grids should be sufficient; the guidelines [96-98] can be adopted. The results of the grid convergence study should be uniformly reported using the Grid Convergence Index (GCI) by Roache [200,201]. An example of grid convergence analysis and application of the GCI for natural ventilation of a generic isolated building is shown in Figure 19.

5.9. Perform an appropriate validation study

The AIAA defines validation as [267]: “*The process of determining the degree to which a model is an accurate representation of the real world from the perspective of the intended uses of the model.*” It refers to quantifying uncertainties in CFD, including input uncertainty (by sensitivity analysis and uncertainty analysis) and quantifying physical modeling uncertainty (by comparison of CFD results with high-quality experiments) [268-270]. Oberkampf and Trucano [268] correctly state that meaningful validation is only possible after good quantitative estimates have been obtained of all numerical errors, the input uncertainty and the uncertainty of the experimental data used for validation.

In many cases in urban physics, experimental data for the case under study will not be available. In this case, the advice is to perform sub-configuration validation, which consists of subdividing the actual configuration into a number of generic sub-configurations, each of which contains one or several of the salient flow features in the actual configuration (e.g. [49,97,224,269]). For generic sub-configurations, several high-quality experimental data sets are available in the published literature and/or online (e.g. the CEDVAL database of the University of Hamburg (www.mi.uni-hamburg.de/cedval), the data sets by the Architectural Institute of Japan (http://www.aij.or.jp/jpn/publish/cfdguide/index_e.htm) or the CODASC database of the Karlsruhe Institute of Technology (<http://www.ifh.uni-karlsruhe.de/science/aerodyn/CODASC.htm>) which are then used for CFD validation. When a given combination of computational parameters and settings provides accurate simulation results for each of the sub-configurations, it can reasonably be assumed that the same or a similar combination will also provide accurate results for the actual configuration. However, also for the sub-configuration validation case, first the numerical errors, input uncertainty and the uncertainty of the experimental data should be assessed. This is a tedious procedure, but it is essential if the quality of the modeling process is to be maintained.

5.10. Report essential elements of the modeling process

Strictly, all components and steps of a CFD simulation should be reported, in such a way that the simulation, when repeated by someone else, would yield exactly the same results. Given the very large complexity of CFD simulations in urban physics and the very wide range of numerical and physical parameters, complete reporting is not straightforward. Even reporting of the grid topology alone can be very tedious. Therefore, at least the most important modeling choices should be reported in detail, following best practice guidelines such as mentioned in section 4.3 and in the present paper. In addition, the results of grid convergence analysis, other verification efforts and validation efforts should be reported in a quantitative way (“good” agreement is not an acceptable report of a validation study).

6. Summary and conclusions

Urban physics is the science and engineering of physical processes in urban areas. It basically refers to the transfer of heat and mass in the outdoor and indoor urban environment, and its interaction with humans, fauna, flora and materials. Urban physics is a rapidly increasing focus area as it is key to understanding and addressing the grand societal challenges climate change, energy, health, security, transport and aging. The main assessment tools in urban physics are field measurements, full-scale and reduced-scale laboratory measurements and numerical simulation methods including Computational Fluid Dynamics (CFD). In the past 50 years, CFD has undergone a successful transition from an emerging field into an increasingly established field in urban physics research, practice and design.

This review and position paper addresses Computational Fluid Dynamics (CFD) for urban physics. It consists of two parts. In the first part, the importance of urban physics related to the grand societal challenges is described, after which the spatial and temporal scales in urban physics and the associated model categories are outlined. In the second part, based on a brief theoretical background, some views on CFD are provided. Possibilities and limitations are discussed, and in particular, ten tips and tricks towards accurate and reliable CFD simulations are presented. These tips and tricks are certainly not intended to be complete, rather they are intended to complement existing CFD best practice guidelines on ten particular aspects.

The importance of urban physics is rapidly increasing. The continuing urbanization amplifies the grand challenges in terms of energy, health, security, transport and aging, many of which are interrelated and all of which are increasingly pertaining to urban areas. These grand challenges give rise to a large number of specific and important focus areas in urban physics, ranging from thermal environment, pollutant dispersion and pedestrian-level wind conditions over meteorological phenomena to wind loads on buildings, vehicles, windborne debris, fire and acoustics.

In terms of spatial scales, urban physics is mainly practiced at the meteorological microscale and the building scale. However, as all scales are interrelated, connected and partially overlapping, and as the end focus in urban physics will often be the human, section 3 has presented the range of spatial (and temporal) scales pertaining to urban physics in its widest sense: from the meteorological macroscale, mesoscale and microscale to the building scale, the building component scale and the scale of humans and materials. In addition, the related model categories have been outlined. The model category belonging to the meteorological microscale and the building scale (outdoor environment) is CFD. Therefore, the remainder of the paper focuses on CFD for urban physics.

CFD for urban physics is based on different approximate forms of the governing equations, yielding different approaches: RANS, URANS, hybrid URANS/LES and LES. Although steady RANS is associated with quite important limitations in terms of modeling important features of the fully turbulent flow around bluff bodies in urban physics, still, it is by far the most widely used approach in most urban physics focus areas. The reason for this is twofold: (i) the computational expense of LES and (ii) the increased model complexity of LES in combination with the absence of extensive best practice guidelines for LES. Such best practice guidelines exist for RANS, as they have been developed in the past 15 years. This paper cites most of these guidelines, because the establishment of these guidelines has been an important step towards more accurate and reliable CFD simulations in urban physics.

Based on the very important and very valuable efforts that have led to the present best practice guidelines in CFD, this paper presents ten particular tips and tricks to complement these guidelines. Some of these are new suggestions, such as the directional blockage ratio, while others are drawn from previous papers by the author and his co-workers, such as the surface-grid extrusion technique, and yet others are a combination of new insights and earlier work, such as the specification of appropriate roughness parameters. These tips and tricks are intended to contribute to more accurate and reliable CFD simulations.

In view of the continuing urbanization and the societal grand challenges, the discipline of urban physics has never been more important than it is today. It is also rapidly expanding as other disciplines are joining forces with the current urban physicists by shifting the focus of the efforts in their discipline towards buildings and urban areas. On the meteorological microscale and the building scale (outdoor environment), CFD is the most important numerical simulation approach. Further increases in computational resources will allow upscaling and downscaling of CFD capabilities, as well as paving a more viable way towards practical use of LES. Nevertheless, many concerted efforts and many years will be needed to develop extensive and internationally accepted best practice guidelines for LES in urban physics, as now exist for RANS. In addition, validation with high-quality experimental data will remain indispensable for a very long time to come, and should continue to accompany further developments in and applications of CFD.

7. Acknowledgments

The author is greatly indebted to his three mentors in Building Physics, in alphabetical order of last name: Prof.dr.ir. Jan Carmeliet, previously full professor at Leuven University in Flanders, Belgium and now Chair of Building Physics at ETH Zurich, Switzerland, Prof.dr.ir. Hugo Hens, emeritus full professor at Leuven University, Flanders, Belgium and Prof.dr.ir. Jan Hensen, full professor at Eindhoven University in the Netherlands. The author is also greatly indebted to his mentor in Wind Engineering and Computational Wind Engineering, Prof.dr. Ted Stathopoulos, whose Building Aerodynamics Laboratory at Concordia University in Montreal he joined in 2004-2005, thanks to a postdoctoral fellowship from the Research Fund – Flanders (FWO-Vlaanderen). During the review process of this paper, it has become known that Eindhoven University of Technology will award its prestigious 2015 Honorary Doctorate in Science and Engineering to Prof.dr. Ted Stathopoulos, upon recommendation by the author. The author is also deeply indebted to his mentor in Applied Physics, Prof.dr.ir. GertJan van Heijst, full professor at the Department of Applied Physics at Eindhoven University of Technology.

The author is very grateful to Prof.dr.ir. Qingyan (Yan) Chen, Editor-in-Chief of Building and Environment and to the colleagues at Elsevier: Joe d'Angelo, Louise Curtis, Ann Gabriel, Laure Ballu and Maggie Yang. This Golden Issue celebrates 50 years of the journal Building & Environment. But even more remarkable than the 50 year anniversary is the transformation that this journal has undergone in the past few years, in which it has become the top international journal that it is today, consistently recruiting the very best papers from the very best scientists in our field.

The author expresses his gratitude to the postdocs, PhD students and MSc students in his group in Urban Physics and Environmental Wind Engineering at Eindhoven University of Technology in the Netherlands and at Leuven University in Flanders, Belgium. The most rewarding and most enjoyable aspect of the job is the opportunity to work with and educate excellent young individuals. Special thanks therefore go to current postdocs dr.ir. Twan van Hooff and dr. Ivo Kalkman, and to former postdoc dr. Christof Gromke. Special thanks also go to former PhD students dr.ir. Pierre Gousseau, dr.ir. Twan van Hooff (*cum laude PhD degree at Eindhoven University*), dr.ir. Rubina Ramponi (*cum laude PhD degree at Politecnico di Milano*), dr. Aytac Kubilay (ETH Zurich), and to current PhD students Hamid Montazeri, Wendy Janssen, Okke Bronkhorst, Thijs van den Brande (KU Leuven), Yasin Toparlar, Adelya Khayrullina, Jorge Isaac Peren Montero, Antonio Castillo Torres, Katarina Kosutova, Raffaele Vasaturo, Samy Iousef, Fabio Malizia, Feiyu Geng, Michiel Ritzen, Alessio Ricci, Olga Palusci and Antoniou Nestoras. The same warm acknowledgment is given to PDEng student Argyrios Papadopoulos.

References

1. AMS. Meteorological Glossary. American Meteorological Society; 2014. <http://glossary.ametsoc.org/wiki/Mesoscale>. Retrieved on March 4, 2014.
2. UN. United Nations Department of Economic and Social Affairs, Population Division; 2014. World Urbanization Prospects: The 2014 Revision, Highlights (ST/ESA/SER.A/352).
3. UN. United Nations. <http://www.un.org/en/development/desa/population/theme/urbanization/>, retrieved on December 29, 2014.
4. IPCC. Climate Change 2014. International Panel on Climate Change. Fifth Assessment Report.
5. European Commission. 2014. Adaptation to climate change; 2014. http://ec.europa.eu/clima/policies/adaptation/index_en.htm. Retrieved on December 28, 2014.
6. IEA. World Energy Outlook 2008. International Energy Agency. ISBN: 978-92-64-04560-6; 2008.
7. Haines A, Kovats RS, Campbell-Lendrum D, Corvalan C. Climate change and human health: impacts, vulnerability and public health. *Public Health* 2006;120:585-96.
8. Watkiss P. Final Report. The ClimateCOST project, vol. 1. Europe: Stock Environ Inst; 2011.
9. Xu P, Huang YJ, Miller N, Schlegel N, Shen P. Impacts of climate change on building heating and cooling energy patterns in California. *Energy* 2012;44:792-804.
10. Changnon SA, Kunkel EK, Reinke BC. Impacts and responses to the 1995 heat wave: a call to action. *Bull Am Meteorol Soc* 1996;77:1497-506.
11. Garssen J, Harmsen C, de Beer J. Effect of the summer 2003 heat wave on mortality in the Netherlands. *Eurosurveillance* 2005;10:165-7.
12. Conti S, Meli P, Minelli G, Solimini R, Toccaceli V, Vichi M, et al. Epidemiologic study of mortality during the summer 2003 heat wave in Italy. *Environ Res* 2005;98:390-9.
13. Awbi HB. Ventilation of buildings. London, UK: Spon Press; 2003.
14. Sarraat C, Lemonsu, Masson V, Guedalia D. Impact of urban heat island on regional atmospheric pollution. *Atmos Environ* 2006;40:1743-58.
15. Tan J, Zheng Y, Tang X, Guo C, Li L, Song G, et al. The urban heat island and its impact on heat waves and human health in Shanghai. *Int J Biometeorol* 2010;54:75-84.
16. Memon RA, Leung DYC, Liu C-H, Leung MKH. Urban heat island and its effect on the cooling and heating demands in urban and suburban areas of Hong Kong. *Theor Appl Climatol* 2010;103:441-50.
17. Emmanuel R, Krüger EL. Urban heat island and its impact on climate change resilience in a shrinking city: the case of Glasgow, UK. *Build Environ* 2012;53:137-49.
18. Kolokotroni M, Ren X, Davies M, Mavrogianni A. London's urban heat island: impact on current and future energy consumption in office buildings. *Energy Build* 2012;47:302-11.
19. Toparlar Y, Blocken B, Vos P, van Heijst GJF, Janssen WD, van Hooff T, Montazeri H, Timmermans HJP. CFD simulation and validation of urban microclimate: A case study for Bergpolder Zuid, Rotterdam. *Build Environ* 2015; 83:79-90.
20. IEA. World Energy Outlook 2014 (WEO-2014). International Energy Agency. Executive Summary; 2014.
21. <http://www.iea.org/publications/scenariosandprojections/>. Retrieved on December 29, 2014
22. United Nations Environment Programme UNEP. Sustainable Buildings and Climate Initiative. <http://www.unep.org/sbci/>. Retrieved on December 29, 2014.

¹⁶ “The base of every state is the education of the youth”. Pythagoras of Samos (c. 570 BC – c. 495 BC), Greek philosopher and mathematician.

23. WHO. http://www.who.int/topics/urban_health/en/. Retrieved on December 29, 2014. World Health Organization.
24. WHO. Global health risks: mortality and burden of disease attributable to selected major risks. World Health Organization, Geneva, 2009.
25. WHO. Why urban health matters. 1000 cities, 1000 lives. World Health Day 2010. World Health Organization; 2010.
26. ISECOM. <http://www.isecom.org/>. Retrieved on December 29, 2014.
27. UNDP. Human Development Report 1994. United Nations Development Program. Oxford University Press; 1994.
28. Fuglestad J, Berntsen T, Myhre G, Rypdal K, Bleilvedt Skele R. Climate forcing from the transport sectors. PNAS 2007;105(2): 454-458.
29. WHO. <http://www.who.int/ageing/about/facts/en/>. Retrieved on December 29, 2014.
30. Murakami, S., Ooka, R., Mochida, A., Yoshida, S., Kim, S. CFD analysis of wind climate from human scale to urban scale. J Wind Eng Ind Aerodyn, 1999;81(1-3):57-81.
31. Stathopoulos, T. Pedestrian level winds and outdoor human comfort. J Wind Eng Ind Aerodyn 2006;94(11):769-780.
32. Mochida A, Lun IYF. Prediction of wind environment and thermal comfort at pedestrian level in urban area. J Wind Eng Ind Aerodyn, 2008;96 (10-11):1498-1527.
33. Moonen, P., Defraeye, T., Dorer, V., Blocken B, Carmeliet, J. Urban Physics: Effect of the micro-climate on comfort, health and energy demand. Frontiers of Architectural Research 2012;1(3):197-228.
34. Lee RL, Albritton JR, Ermak DL, Kim J. Computational fluid dynamics modeling for emergency preparedness and response. Environmental Modelling and Software 1997;12(1):43-50.
35. Vardoulakis S, Fisher BEA, Pericleous K, Gonzalez-Flesca N. Modelling air quality in street canyons: a review. Atmos Environ 2003;37(2):155-182.
36. Canepa E. An overview about the study of downwash effects on dispersion of airborne pollutants. Environmental Modelling and Software 2004;19(12):1077-1087.
37. Meroney RN. Wind tunnel and numerical simulation of pollution dispersion: a hybrid approach. Paper for Invited Lecture at the Croucher Advanced Study Institute, Hong Kong University of Science and Technology, 6-10 December 2004.
38. Li XX, Liu CH, Leung DY, Lam KM. Recent progress in CFD modelling of wind field and pollutant transport in street canyons. Atmos Environ 2006;40(29):5640-5658.
39. Tominaga Y, Stathopoulos T. Turbulent Schmidt numbers for CFD analysis with various types of flowfield. Atmos Environ 2007;41(37):8091-8099.
40. Fernando HJS, Zajic D, Di Sabatino S, Dimitrova R, Hedquist B, Dallman A. Flow, turbulence and pollutant dispersion in urban atmospheres. Physics of Fluids 2010;22(5):051301.
41. Gousseau P, Blocken B, Stathopoulos T, van Heijst GJF. CFD simulation of near-field pollutant dispersion on a high-resolution grid: a case study by LES and RANS for a building group in downtown Montreal. Atmos Environ 2011;45(2):428-438.
42. Blocken B, Stathopoulos T, Carmeliet J, Hensen JLM. Application of CFD in building performance simulation for the outdoor environment: an overview. Journal of Building Performance Simulation 2011;4(2):157-184.
43. Tominaga Y, Stathopoulos T. CFD simulation of near-field pollutant dispersion in the urban environment: A review of current modelling techniques. Atmos Environ 2013;79:716-730.
44. Di Sabatino S, Buccolieri R, Salizzoni P. Recent advancements in numerical modelling of flow and dispersion in urban areas: a short review. Int. J. Environment and Pollution 2013;52(3-4):172-191.
45. Blocken B, Tominaga Y, Stathopoulos T. Editorial to virtual special issue: CFD simulation of micro-scale pollutant dispersion in the built environment. Build Environ 2013;64:225-230.
46. Xia Q, Niu J, Liu X. Dispersion of air pollutants around buildings: A review of past studies and their methodologies. Indoor and Built Environment 2014; 23(2):201-224.
47. Blocken B, Carmeliet, J. Pedestrian wind environment around buildings: Literature review and practical examples. Journal of Thermal Envelope and Building Science 2004;28(2):107-159.
48. Yoshie R, Mochida A, Tominaga Y, Kataoka H, Harimoto K, Nozu T, Shirasawa T. Cooperative project for CFD prediction of pedestrian wind environment in the Architectural Institute of Japan. J Wind Eng Ind Aerodyn 2007;95(9-11):1551-1578.
49. Blocken B, Janssen WD, van Hooff T. CFD simulation for pedestrian wind comfort and wind safety in urban areas: General decision framework and case study for the Eindhoven University campus. Environmental Modelling and Software 2012;30:15-34.
50. Blocken B, Stathopoulos, T. Editorial to virtual special issue: CFD simulation of pedestrian-level wind conditions around buildings: past achievements and prospects. J Wind Eng Ind Aerodyn 2013;121:138-145.
51. Blocken B. 50 years of Computational Wind Engineering: Past, present and future. J Wind Eng Ind Aerodyn 2014;129: 69-102.

52. Stathopoulos T. Computational Wind Engineering: Past achievements and future challenges. *J Wind Eng Ind Aerodyn* 1997;67-68:509-532.
53. Tamura T. Reliability on CFD estimation for wind-structure interaction problems. *J Wind Eng Ind Aerodyn*, 1999;81:117-143.
54. Stathopoulos T. Wind loads on low buildings: in the wake of Alan Davenport's contributions. *J Wind Eng Ind Aerodyn* 2003;91(12-15):1565-1585.
55. Kareem A. Numerical simulation of wind effects: A probabilistic perspective. *J Wind Eng Ind Aerodyn*, 2008;96(10-11):1472-1497.
56. Ge YJ, Xiang HF. 2008. Recent development of bridge aerodynamics in China. *J Wind Eng Ind Aerodyn*, 96, 6-7, 736-768.
57. Baker CJ. The flow around high speed trains. *J Wind Eng Ind Aerodyn* 2010;98(6-7):277-298.
58. Blocken B, Carmeliet J. A review of wind-driven rain research in building science. *J Wind Eng Ind Aerodyn*, 2004;92(13):1079-1130.
59. Blocken B, Carmeliet J. Overview of three state-of-the-art wind-driven rain assessment models and comparison based on model theory. *Build Environ* 2010;45(3):691-703.
60. Blocken B, Derome D, Carmeliet J. Rainwater runoff from building facades: a review. *Build Environ* 2013;60:339-361.
61. Richards PJ, Williams N, Laing B, McCarty M, Pond M. Numerical calculation of the three-dimensional motion of wind-borne debris. *J Wind Eng Ind Aerodyn* 2008;96(10-11): 2188-2202.
62. Holmes JD. Windborne debris and damage risk models: a review. *Wind Struct* 2010;13(2):95-108.
63. Richards PJ. Dispersion of windborne debris. *J Wind Eng Ind Aerodyn* 2012;104:594-602.
64. Hargreaves DM, Kakimpa B, Owen JS. The computational fluid dynamics modelling of the autorotation of square, flat plates. *Journal of Fluids & Structures* 2014;46:111-133.
65. de Wilde P, Coley D. The implications of a changing climate for buildings. *Build Environ* 2012;55:1-7.
66. Albers RAW, Bosch PR, Blocken B, van den Dobbelsteen AAJF, van Hove LWA, Spit TJM, van de Ven F, van Hooft T, Rovers V. Overview of challenges and achievements in the Climate Adaptation of Cities and in the Climate Proof Cities program. *Build Environ* 2015;83:1-10.
67. Reichrath S, Davies TW. Using CFD to model the internal climate of greenhouses: past, present and future. *Agronomie* 2002;22:3-19.
68. Karava P, Stathopoulos T, Athienitis AK. Wind driven flow through openings—a review of discharge coefficients. *Int J Vent* 2004;3:255-266.
69. Norton T, Sun DW, Grant J, Fallon R, Dodd V. Applications of computational fluid dynamics (CFD) in the modelling and design of ventilation systems in the agricultural industry: A review. *Bioresource Technology* 2007;98(12):2386-2414.
70. Chen Q. Ventilation performance prediction for buildings: A method overview and recent applications. *Build Environ* 2009;44(4):848-858.
71. Bournet PE, Boulard T. Effect of ventilator configuration on the distributed climate of greenhouses: A review of experimental and CFD studies. *Computers and Electronics in Agriculture* 2010;74(2):195-217.
72. Jiru TE, Bitsuamlak GT. Application of CFD in modelling wind-induced natural ventilation of buildings – a review. *International Journal of Ventilation* 2010;9(2):131-147.
73. Ramponi R, Blocken B. CFD simulation of cross-ventilation for a generic isolated building: impact of computational parameters. *Build Environ*, 2012;53:34-48.
74. Hughes BR, Calautit JK, Ghani SA. The development of commercial wind towers for natural ventilation: a review. *Applied Energy* 2012;92:606-627.
75. Bjerg B, Cascone G, Lee, I.B., Bartzanas, T., Norton, T., Hong, S.W., Seo, I.H., Banhazi, T., Liberati, P., Marucci, A., Zhang, G., Modelling of ammonia emissions from naturally ventilated livestock buildings. Part 3: CFD modelling. *Biosystems Engineering* 2013;116:259-275.
76. Meyer RD, Gang T. An overview of unsteady analysis techniques for natural wind turbulence and its effects on natural ventilation. *International Journal of Ventilation* 2014;13(1):65-76.
77. Peren JJ, van Hooft T, Leite BCC, Blocken B. CFD analysis of cross-ventilation of a generic isolated building with asymmetric opening positions: impact of roof angle and opening location. *Build Environ* 2015;85: 263-276.
78. Takagi, M. Application of computers to automobile aerodynamics. *J Wind Eng Ind Aerodyn*, 1990;33(1-2): 419-428.
79. Hucho, W.H., Sovran, G. Aerodynamics of road vehicles. *Annual Review of Fluid Mechanics* 1993;25:485-537.
80. Mueller, T.J., DeLaurier, J.D. Aerodynamics of small vehicles. *Annual Review of Fluid Mechanics*, 2003;35:89-111.
81. Katz, J. Aerodynamics of race cars. *Annual Review of Fluid Mechanics* 2006;38:27-63.
82. Ayotte, K. Computational modelling for wind energy assessment. *J Wind Eng Ind Aerodyn*, 2008;96(10-11):1571-1590.

83. Sumner, J., Watters, C.S., Masson, C. CFD in wind energy: the virtual, multiscale wind tunnel. *Energies* 2010;3:989-1013.
84. Sorensen, J.N. Aerodynamic aspects of wind energy conversion. *Annual Review of Fluid Mechanics* 2011;43:427-448.
85. Roy, S., Saha, U.K. Review on the numerical investigations into the design and development of Savonius wind rotors. *Renewable and Sustainable Energy Reviews* 2013;24:73-83.
86. Tagliafico LA, Scarpa F, De Rosa M. Dynamic thermal models and CFD analysis for flat-plate thermal solar collectors – A review. *Renewable and Sustainable Energy Reviews* 2014;30:526-537.
87. Lupi F, Borri C, Harte R, Krätzig WB, Niemann HJ. Facing technological challenges of solar updraft power plants. *Journal of Sound and Vibration* 2015;334:57-84.
88. Vennell R, Funke SW, Draper S, Stevens C, Divett T. Designing large arrays of tidal turbines: A synthesis and review. *Renewable and Sustainable Energy Reviews* 2015;41: 454-472.
89. Berglund B, Hassmen P, Job RFS. Sources and effects of low-frequency noise. *Journal of the Acoustical Society of America* 1996;99(5):2985-3002.
90. Ouis D. Annoyance from road traffic noise: A review. *Journal of Environmental Psychology* 2001;21(1):101-120.
91. De Salis MHF, Oldham DJ, Sharples S. Noise control strategies for naturally ventilated buildings. *Build Environ* 2002;37(5):471-484.
92. Zhang M, Kang J. Towards the evaluation, description, and creation of soundscapes in urban open spaces. *Environment and Planning B – Planning & Design*. 2007;34(1):68-86.
93. Pirrear S, De Valck E, Cluydts R. Nocturnal road traffic noise: A review on its assessment and consequences on sleep and health. *Environment International* 2010;36(5):492-498.
94. Hornikx M, Forssen J. Modelling of sound propagation to three-dimensional urban courtyards using the extended Fourier PSTD method. *Applied Acoustics* 2011;72(9):665-676.
95. Tominaga, Y., Okaze, T., Mochida, A. CFD modeling of snowdrift around a building: An overview of models and evaluation of a new approach. *Build Environ* 2011;46(4):899-910.
96. Franke, J., Hirsch, C., Jensen, A.G., Krüs, H.W., Schatzmann, M., Westbury, P.S., Miles, S.D., Wisse, J.A., Wright, N.G. Recommendations on the use of CFD in wind engineering. In: van Beeck, J.P.A.J. (Ed.), *Proceedings of the International Conference on Urban Wind Engineering and Building Aerodynamics. COST Action C14, Impact of Wind and Storm on City Life Built Environment*. Von Karman Institute, Sint-Genesius-Rode, Belgium, 5–7 May 2004.
97. Franke, J., Hellsten, A., Schlünzen, H., Carissimo, B. (Eds.). *Best practice guideline for the CFD simulation of flows in the urban environment*. COST Office Brussels, ISBN 3-00-018312-4; 2007.
98. Tominaga, Y., Mochida, A., Yoshie, R., Kataoka, H., Nozu, T., Yoshikawa, M., Shirasawa, T. AIJ guidelines for practical applications of CFD to pedestrian wind environment around buildings. *J Wind Eng Ind Aerodyn* 2008;96(10-11):1749-1761.
99. Tamura, T. Towards practical use of LES in wind engineering. *J Wind Eng Ind Aerodyn* 2008;96(10-11):1451-1471.
100. Tamura, T., Nozawa, K., Kondo, K. AIJ guide for numerical prediction of wind loads on buildings. *J Wind Eng Ind Aerodyn* 2008;96 (10-11):1974-1984.
101. Tabor, G.R., Baba-Ahmadi, M.H. Inlet conditions for large eddy simulation: A review. *Computers and Fluids* 2010;39(4):553-567.
102. Franke, J., Hellsten, A., Schlünzen, H., Carissimo, B. The COST 732 best practice guideline for CFD simulation of flows in the urban environment – A summary. *International Journal of Environmental Pollution* 2011;44(1-4):419-427.
103. Murakami, S. Computational Wind Engineering. *J Wind Eng Ind Aerodyn* 1990;36(1):517-538.
104. Murakami, S. Comparison of various turbulence models applied to a bluff body. *J Wind Eng Ind Aerodyn*, 1993;46&47:21-36.
105. Murakami, S. Current status and future trends in computational wind engineering. *J Wind Eng Ind Aerodyn* 1997;67&68:3-34.
106. Murakami, S. Overview of turbulence models applied in CWE-1997. *J Wind Eng Ind Aerodyn* 1998;74-76:1-24.
107. Ferziger, J.H. Approaches to turbulent flow computation: applications to flow over obstacles. *J Wind Eng Ind Aerodyn* 1990;35:1-19.
108. Ferziger, J.H. A computational fluid dynamicist's view of CWE. *J Wind Eng Ind Aerodyn*, 1993;46–47:879-880.
109. Ferziger, J.H. Simulation of complex turbulent flows: recent advances and prospects in wind engineering. *J Wind Eng Ind Aerodyn*, 1993;46–47:195-212.
110. Leschziner, M.A. Modelling engineering flows with Reynolds stress turbulence closure. *J Wind Eng Ind Aerodyn* 1990;35:21-47.

111. Leschziner M.A. Computational modelling of complex turbulent flow - expectations, reality and prospects. *J Wind Eng Ind Aerodyn* 1993;46–47:37-51.
112. Hughes, T.J.R, Jansen, K., Finite element methods in wind engineering. *J Wind Eng Ind Aerodyn*, 1993;46–47:297-313.
113. Shah, K.B., Ferziger, J.H. A fluid mechanics view of wind engineering: Large eddy simulation of flow past a cubic obstacle. *J Wind Eng Ind Aerodyn*, 1997;67–68:211-224.
114. Stathopoulos, T. The numerical wind tunnel for industrial aerodynamics: real or virtual in the new millennium? *Wind and Structures*, 2002;5 (2–4):193–208.
115. Rodi, W. Comparison of LES and RANS calculations of the flow around bluff bodies. *J Wind Eng Ind Aerodyn*, 1997;69–71:55-75.
116. Tamura, T., Kawai, H., Kawamoto, S., Nozawa, K., Sakamoto, S., Ohkuma, T. Numerical prediction of wind loading on buildings and structures – Activities of AIJ cooperative project on CFD. *J Wind Eng Ind Aerodyn*, 1997;67-68:671-685.
117. Gosman, A.D. Developments in CFD for industrial and environmental applications in wind engineering. *J Wind Eng Ind Aerodyn* 1999;81(1–3):21-39.
118. Castro, I.P., Graham, J.M.R. Numerical wind engineering: the way ahead? *Proceedings of the Institution of Civil Engineers – Structures and Buildings* 1999;134(3):275-277.
119. Tezduyar, T.E. CFD methods for three-dimensional computation of complex flow problems. *J Wind Eng Ind Aerodyn* 1999;81(1–3):97-116.
120. Fujii, K. Progress and future prospects of CFD in aerospace—Wind tunnel and beyond. *Progress in Aerospace Sciences* 2005;41(6):455-470.
121. Norton, T., Sun, D.W., Computational fluid dynamics (CFD) – an effective and efficient design and analysis tool for the food industry: a review. *Trends in Food Science & Technology* 2006;17:600-620.
122. Bartzis, J.G. Turbulence modelling in the atmospheric boundary layer: a review and some recent developments. *WIT Transactions on Ecology and the Environment: Air Pollution* 2006;XIV:86:3-12.
123. Baker C.J., Wind engineering – Past, present and future. *J Wind Eng Ind Aerodyn* 2007;95(9-11):843-870.
124. Hanjalic, K., Will RANS survive LES? A view of perspectives. *Journal of Fluids Engineering – Transactions of the ASME* 2004;127(5):831-839.
125. Hanjalic, K., Kenjeres, S. Some developments in turbulence modeling for wind and environmental engineering. *J Wind Eng Ind Aerodyn* 2008;96(10-11):1537-1570.
126. Squires, K.D., Krishnan, V., Forsythe, J.R. Prediction of the flow over a circular cylinder at high Reynolds number using detached-eddy simulation. *J Wind Eng Ind Aerodyn*, 2008;96(10–11):1528-1536.
127. Cochran, L., Derickson R. A physical modeler's view of Computational Wind Engineering. *J Wind Eng Ind Aerodyn* 2011;99(4):139-153.
128. Blocken B, Gualtieri, C. Ten iterative steps for model development and evaluation applied to Computational Fluid Dynamics for Environmental Fluid Mechanics. *Environmental Modelling and Software* 2012;33:1-22.
129. AMS. Glossary of meteorology. American Meteorological Society. <http://glossary.ametsoc.org>. Retrieved on December 30, 2014.
130. Schlünzen, K.H., Grawe, D., Bohnenstengel, S.I., Schlüter, I., Koppmann, R. Joint modelling of obstacle induced and mesoscale changes—Current limits and challenges. *J Wind Eng Ind Aerodyn*, 2011;99(4):217-225.
131. Orlanski I. A rational subdivision of scales for atmospheric processes. *Bulletin of the American Meteorological Society* 1975;56(5):527–530.
132. Richardson, L.F. *Weather prediction by numerical process*. Cambridge, The University Press; 1922.
133. Charney, J.G. The use of the primitive equations of motion in numerical prediction. *Tellus* 1955;7:22-26.
134. Chapman S. *Introduction to Dover edition of weather prediction by numerical process*; 1965.
135. Lynch, P. The emergence of numerical weather prediction: Richardson's dream. Cambridge University Press, Cambridge, UK, pp. 1-27; 2006.
136. Lynch, P. The origins of computer weather prediction and climate modelling. *Journal of Computational Physics* 2008; 227:3431-3444.
137. Orville HD. Recovery of pressure field in mesoscale numerical models. *Bulletin of the American Meteorological Society* 1967;48(11):837-&.
138. Lavoie RL. Mesoscale numerical model of lake-effect storms. *Journal of the Atmospheric Sciences* 1972;29(6):1025-&.
139. Dudhia J. Numerical study of convection observed during the winter monsoon experiment using a mesoscale two-dimensional model. *Journal of the Atmospheric Sciences* 1989;46(20):3077-3107.

140. Pielke RA, Cotton WR, Walko RL, Tremback CJ, Lyons WA, Grasso LD, Nicholls ME, Moran MD, Wesley DA, Lee TJ, Copeland JH. A comprehensive meteorological modeling system – RAMS. *Meteorology and Atmospheric Physics* 1992;49(1-4):69-91.
141. Black TL. The new NMC mesoscale Eta-model. *Description and forecast examples. Weather and Forecasting* 1994;9(2):265-278.
142. Chen F, Dudhia J. Coupling an advanced land surface-hydrology model with the Penn State-NCAR MM5 modeling system. Part I: Model implementation and sensitivity. *Monthly Weather Review* 2001;129(4):569-585.
143. Yamada T, Koike K. Downscaling mesoscale meteorological models for computational wind engineering applications. *J Wind Eng Ind Aerodyn* 2011;99(4): 99-216.
144. Hoffman FM, Hargrove WW, Drake JB, Mac Post W. ORNL Booth Material for SuperComputing '99 Regional Climate Modeling and Multivariate Geographic Clustering. http://www.climate modeling.org/~forrest/presentations/Hoffman_SC99-ORNL_1999/ Retrieved on December 30, 2014; 1999.
145. Mochida A, Iizuka S, Tominaga Y, Lun IYF. Up-scaling CWE models to include mesoscale meteorological influences. *J Wind Eng Ind Aerodyn* 2011;99(4):187-198.
146. Chow WK. Application of computational fluid dynamics in building services engineering. *Build Environ* 1996;31(5):425-436.
147. Liu X, Zhai Z. Inverse modeling methods for indoor airborne pollutant tracking: literature review and fundamentals. *Indoor Air* 2007;17(6):419-438.
148. Li Y, Nielsen PV. Commemorating 20 years of indoor air CFD and ventilation research. *Indoor Air* 2011;21(6):442-453.
149. Crawley DB, Lawrie LK, Winkelmann FC, Buhl WF, Huang YJ, Pedersen CO, Strand RK, Liesen RJ, Fisher DE, Witte MJ, Glazer J. EnergyPlus: creating a new-generation building energy simulation program. *Energy and Buildings* 2001;33(4):319-331.
150. Citherlet S, Clarke JA, Hand J. Integration in building physics simulation. *Energy and Buildings* 2001;33(5):451-461.
151. Crawley DB, Hand JW, Kurnmerr M, Griffith BT. Contrasting the capabilities of building energy performance simulation programs. *Build Environ* 2008;43(4):661-673.
152. Costola D, Blocken B, Hensen JLM. Overview of pressure coefficient data in building energy simulation and airflow network programs. *Build Environ* 2009;44(10):2027-2036.
153. Hoes P, Hensen JLM, Loomans MGLC, de Vries B, Bourgeois D. User behavior in whole building simulation. *Energy and Buildings* 2009;41(3):295-302.
154. Trcka M, Hensen JLM. Overview of HVAC system simulation. *Automation in Construction* 2010;19(2):93-99.
155. Hopfe CJ, Hensen JLM. Uncertainty analysis in building performance simulation for design support. *Energy and Buildings* 2011;43(10):2798-2805.
156. Bartak M, Beausoleil-Morrison I, Clarke JA, Denev J, Drkal F, Lain M, MacDonald IA, Melikov A, Popiolek Z, Stankov P. Integrating CFD and building simulation. *Build Environ* 2002;37(8-9):865-871.
157. Beausoleil-Morrison I. The adaptive conflation of computational fluid dynamics with whole-building thermal simulation. *Energy and Buildings* 2002;34(9):857-871.
158. Cunningham MJ. Modelling of moisture transfer in structures – I. A description of a finite-difference nodal model. *Build Environ* 1990;25(1): 55-61.
159. Pedersen CR. Prediction of moisture transfer in building constructions. *Build Environ* 1992;27(3):387-397.
160. Hens H. Heat, air and moisture transfer in insulated envelope parts: modelling. International Energy Agency, Annex 24. Final report, volume 1. Acco, Leuven. 1996.
161. Künzle HM, Kiessl K. Calculation of heat and moisture transfer in exposed building components. *Int J Heat Mass Transfer* 1997;40(1):159-167.
162. Hall C, Hoff WD. Water transport in brick, stone and concrete. Spon Press, London and New York; 2002.
163. Hens SLC. Building Physics – Heat, Air and Moisture. Wiley. Ernst and Sohn; 2007.
164. Janssen H, Blocken B, Carmeliet J. Conservative modelling of the moisture and heat transfer in building components under atmospheric excitation. *International Journal of Heat and Mass Transfer* 2007;50(5-6):1128-1140.
165. Blocken B, Roels S, Carmeliet J. A combined CFD-HAM approach for wind-driven rain on building facades. *J Wind Eng Ind Aerodyn* 2007;95(7): 585-607.
166. Steeman HJ, Van Belleghem M, Janssens A, De Paepe M. Coupled simulation of heat and moisture transport in air and porous materials for the assessment of moisture related damage. *Build Environ* 2009;44(10):2176-2184.
167. Van Belleghem M, Steeman M, Janssens H, Janssens A, De Paepe M. Validation of a coupled heat, vapour and liquid moisture transport model for porous materials implemented in CFD. *Build Environ* 2014;81:340-353.

168. Steeman M, Janssens A, Steeman HJ, Van Belleghem M, De Paepe M. On coupling 1D non-isothermal heat and mass transfer in porous materials with a multizone building energy simulation model. *Build Environ* 2010;45(4):865-877.
169. Fiala, D. Dynamic simulation of human heat transfer and thermal comfort. PhD thesis. De Montfort University, Leicester, UK; 1998.
170. Fiala D, Lomas KJ, Stohrer M. A computer model of human thermoregulation for a wide range of environmental conditions: the passive system, *J. Appl. Physiol.* 1999;87:1957-1972.
171. Fiala D, Lomas KJ, Stohrer M. Computer predictions of human thermoregulatory and temperature responses to a wide range of environment conditions. *Int. J. Biometeorol.* 2001;45:143-159.
172. Tanabe S, Kobayashi K, Nakano J, Ozeki Y, Konishi M. Evaluation of thermal comfort using combined multi-node thermoregulation (65MN) and radiation models and computational fluid dynamics (CFD). *Energy and Buildings* 2002;34(6):637-646.
173. Huizenga C, Hui Z. A model of human physiology and comfort for assessing complex thermal environments, *Build. Environ.* 2001;36:691-699.
174. Stolwijk JAJ, Hardy JD. Temperature regulation in man – a theoretical study. *Pflügers Archives*, 1966;291:129-162.
175. Stolwijk JAJ. A mathematical model of physiological temperature regulation in man. NASA, CR-1855, 1971.
176. Murakami S, Kato S, Zeng J. Combined simulation of airflow, radiation and moisture transport for heat release from a human body. *Build Environ* 2000;35(6):489-500.
177. Cropper PC, Yang T, Cook M, Fiala D, Yousaf R. Coupling of a model of human thermoregulation with computational fluid dynamics for predicting human-environment interaction. *Journal of Building Performance Simulation* 2010;3(3):233-243.
178. Ferziger, J.H., Peric, M. Computational methods for fluid dynamics. Springer Berlin, 356p.
179. Bejan, A. 2004. Convection heat transfer. 3rd Ed., Wiley; 1996.
180. Spalart P, Jou WH, Strelets M, Allmaras S. Comments on the feasibility of LES for wings and on the hybrid RANS/LES approach, *Advances in DNS/LES*, 1st AFOSR Int. Conf. on DNS/LES, Gredner Press; 1997.
181. Spalart P, Allmaras S. A one-equation turbulence model for aerodynamic flows. Technical Report AIAA-92-0439, American Institute of Aeronautics and Astronautics; 1992.
182. Jones, W. P., and Launder, B. E. The prediction of laminarization with a 2-equation model of turbulence. *International Journal of Heat and Mass Transfer* 1972;15:301.
183. Yakhot, V., and Orszag, S.A. Renormalization group analysis of turbulence. *Journal of Scientific Computing* 1986;1(1):3-51.
184. Shih, T. H., Liou, W. W., Shabbir, A., and Zhu, J. A new k-ε eddy-viscosity model for high Reynolds number turbulent flows: model development and validation. *Comput Fluids* 1995;24(3):227-238.
185. Wilcox, D. C. Turbulence modelling for CFD, 2nd Ed., DCW Industries, Inc; 2004.
186. Menter, F. Eddy viscosity transport equations and their relation to the k-ε model. *Journal of Fluids Engineering* 1997;119:876-884.
187. Murakami S, Mochida A. Three-dimensional numerical simulation of turbulent flow around buildings using the k-ε turbulence model. *Build Environ* 1989;24(1):51-64.
188. Stathopoulos, T., Baskaran, A. Boundary treatment for the computation of 3D turbulent conditions around buildings. *J Wind Eng Ind Aerodyn*, 1990;35:177-200.
189. Baetke, F., Werner, H., Wengle, H. Numerical simulation of turbulent flow over surface-mounted obstacles with sharp edges and corners. *J Wind Eng Ind Aerodyn*, 1990;35(1-3):129-147.
190. Cowan, I.R., Castro, I.P., Robins, A.G, Numerical considerations for simulations of flow and dispersion around buildings, *J Wind Eng Ind Aerodyn*, 1997;67&68:535-545.
191. Hall, R.C. (ed.). Evaluation of modelling uncertainty. CFD modelling of near-field atmospheric dispersion. Project EMU final report, European Commission Directorate-General XII Science, Research and Development Contract EV5V-CT94- 0531. Surrey: WS Atkins Consultants Ltd; 1997.
192. Schatzmann, M., Rafailidis, S., Pavageau, M. Some remarks on the validation of small-scale dispersion models with field and laboratory data. *J Wind Eng Ind Aerodyn* 1997;67&68: 885-893.
193. Casey, M., Wintergerste, T. Best Practice Guidelines, ERCOFTAC Special Interest Group on Quality and Trust in Industrial CFD, ERCOFTAC, Brussels; 2000.
194. Menter, F., Hemstrom, B., Henriksson, M., Karlsson, R., Latrobe, A., Martin, A., Muhlbauer, P., Scheuerer, M., Smith, B., Takacs, T., Willemsen, S. CFD Best Practice Guidelines for CFD Code Validation for Reactor-Safety Applications, Report EVOLECORR-D01, Contract No. FIKS-CT-2001-00154, 2002.
195. Scaperdas, A., Gilham, S. Thematic Area 4: Best practice advice for civil construction and HVAC, The QNET-CFD Network Newsletter, 2004;2(4):28-33.
196. Bartzis, J.G., Vlachogiannis, D., Sfetsos, A. Thematic area 5: Best practice advice for environmental flows. The QNET-CFD Network Newsletter 2004;2(4):34-39.

197. Britter, R., Schatzmann, M. (Eds.). Model Evaluation Guidance and Protocol Document COST Action 732. COST Office Brussels, ISBN 3-00-018312-4; 2007.
198. Jakeman, A.J., Letcher, R.A., Norton, J.P. Ten iterative steps in development and evaluation of environmental models. *Environmental Modelling and Software* 2006;21(5):602-614.
199. Robson, B.J., Hamilton, D.P., Webster, I.T., Chan, T. Ten steps applied to development and evaluation of process-based biogeochemical models of estuaries. *Environmental Modelling & Software*, 2008;23(4):369-384.
200. Roache, P.J. Perspective – a method for uniform reporting of grid refinement studies. *Journal of Fluids Engineering – Transactions of the ASME* 1994;116(3):405-413.
201. Roache, P.J. Quantification of uncertainty in computational fluid dynamics. *Annual Reviews in Fluid Mechanics* 1997;29:123-160.
202. AIAA. Guide for the verification and validation of computational fluid dynamics simulations, American Institute of Aeronautics and Astronautics, AIAA, AIAA-G-077-1998, Reston, VA; 1998.
203. Oberkampf, W. L., Trucano, T. G., Hirsch, C. Verification, validation, and predictive capability in computational engineering and physics. *Applied Mechanics Reviews* 2004;57(5):345 - 384.
204. Roy, C.J. Review of code and solution verification procedures for computational simulation. *Journal of Computational Physics* 2005;205(1):131-156.
205. Roy, C.J., Oberkampf, W.L. A complete framework for verification, validation, and uncertainty quantification in scientific computing. 48th AIAA Aerospace Sciences Meeting Including the New Horizons Forum and Aerospace Exposition 4 - 7 January 2010, Orlando, Florida; 2010.
206. ASME. Standard for verification and validation in Computational Fluid Dynamics and heat transfer. ASME V&V 20-2009, The American Society of Mechanical Engineers; 2009
207. ASME. <http://journaltool.asme.org/Templates/JFENumAccuracy.pdf>. Retrieved on 30 July 2011.
208. Roache, P.J., Chia, K.N., White, F. Editorial policy statement on the control of numerical accuracy. *Journal of Fluids Engineering*, 1986;108:2
209. Freitas, C.J. *Journal of Fluids Engineering* editorial policy statement on the control of numerical accuracy. *Journal of Fluids Engineering*, 1993;115:339-340.
210. Richards, P.J., Hoxey, R.P. Appropriate boundary conditions for computational wind engineering models using the k- ϵ turbulence model. *J Wind Eng Ind Aerodyn*, 1993;46&47:145-153.
211. Blocken B, Stathopoulos, T., Carmeliet, J. CFD simulation of the atmospheric boundary layer: wall function problems. *Atmos Environ*, 2007;41(2):238-252.
212. Blocken B, Carmeliet, J., Stathopoulos, T. CFD evaluation of wind speed conditions in passages between parallel buildings—effect of wall-function roughness modifications for the atmospheric boundary layer flow. *J Wind Eng Ind Aerodyn*, 2007;95(9-11):941-962.
213. Hargreaves, D.M., Wright, N.G. On the use of the k- ϵ model in commercial CFD software to model the neutral atmospheric boundary layer. *J Wind Eng Ind Aerodyn*, 2007;95(5):355-369.
214. Di Sabatino, S., Buccolieri, R., Pulvirenti, B., Britter, R. Simulations of pollutant dispersion within idealised urban-type geometries with CFD and integral models. *Atmos Environ* 2007;41:8316-8329.
215. Górlé, C., van Beeck, J., Rambaud, P., Van Tendeloo, G. CFD modelling of small particle dispersion: the influence of the turbulence kinetic energy in the atmospheric boundary layer. *Atmos Environ*, 2009;43(3):673-681.
216. Yang, Y., Gu, M., Chen, S., Jin, X. New inflow boundary conditions for modelling the neutral equilibrium atmospheric boundary layer in computational wind engineering. *J Wind Eng Ind Aerodyn*, 2009;97(2):88-95.
217. Parente, A., Górlé, C., van Beeck, J., Benocci, C. Improved k- ϵ model and wall function formulation for the RANS simulation of ABL flows. *J Wind Eng Ind Aerodyn*, 2011;99(4):267-278.
218. Richards, P.J., Norris, S.E. Appropriate boundary conditions for computational wind engineering models revisited. *J Wind Eng Ind Aerodyn*, 2011;99(4):257-266.
219. Tucker, P.G., Mosquera, A. NAFEMS introduction to grid and mesh generation for CFD. NAFEMS CFD Working Group, R0079, 56 pp; 2001.
220. van Hooff, T, Blocken, B. Coupled urban wind flow and indoor natural ventilation modelling on a high-resolution grid: A case study for the Amsterdam ArenA stadium. *Environmental Modelling and Software*, 2010;25(1):51-65.
221. Schatzmann, M., Leidl, B. Issues with validation of urban flow and dispersion CFD models. *J Wind Eng Ind Aerodyn*, 2011;99:169-186.
222. Blocken B, Carmeliet J. Validation of CFD simulations of wind-driven rain on a low-rise building. *Build Environ* 2007;42(7):2530-2548.
223. Blocken B, Moonen P, Stathopoulos T, Carmeliet J. A numerical study on the existence of the Venturi-effect in passages between perpendicular buildings. *Journal of Engineering Mechanics - ASCE* 2008;134(12):1021-1028.

224. Blocken B, Carmeliet J. Pedestrian wind conditions at outdoor platforms in a high-rise apartment building: generic sub-configuration validation, wind comfort assessment and uncertainty issues. *Wind and Structures* 2008;11(1):51-70.
225. Blocken B, Defraeye T, Derome D, Carmeliet J. High-resolution CFD simulations of forced convective heat transfer coefficients at the facade of a low-rise building. *Build Environ* 2009;44(12):2396-2412.
226. Abuku M, Blocken B, Nore K, Thue JV, Carmeliet J, Roels S. On the validity of numerical wind-driven rain simulation on a rectangular low-rise building under various oblique winds. *Build Environ* 2009;44(3):621-632.
227. Nakiboglu G, Gorié C, Horvath I, van Beeck J, Blocken B. Stack gas dispersion measurements with large-scale PIV, aspiration probes and light scattering techniques and comparison with CFD. *Atmos Environ* 43(21): 2009;3396-3406.
228. Briggen PM, Blocken B, Schellen HL. Wind-driven rain on the facade of a monumental tower: numerical simulation, full-scale validation and sensitivity analysis. *Build Environ* 2009;44(8):1675–1690.
229. van Hooff T, Blocken B, Aanen L, Bronsema B. A venturi-shaped roof for wind-induced natural ventilation of buildings: wind tunnel and CFD evaluation of different design configurations. *Build Environ* 2011;46(9):1797-1807.
230. Ramponi R, Blocken B. CFD simulation of cross-ventilation flow for different isolated building configurations: validation with wind tunnel measurements and analysis of physical and numerical diffusion effects. *J Wind Eng Ind Aerodyn* 2012;104-106:408-418.
231. van Hooff T, Blocken B, van Heijst GJF. On the suitability of steady RANS CFD for forced mixing ventilation at transitional slot Reynolds numbers. *Indoor Air* 2013;23(3):236-249.
232. Montazeri H, Blocken B. CFD simulation of wind-induced pressure coefficients on buildings with and without balconies: validation and sensitivity analysis. *Build Environ* 2013;60:137-149.
233. Kubilay A, Derome D, Blocken B, Carmeliet J. CFD simulation and validation of wind-driven rain on a building facade with an Eulerian multiphase model. *Build Environ* 2013;61:69-81.
234. Janssen WD, Blocken B, van Hooff T. Pedestrian wind comfort around buildings: comparison of wind comfort criteria based on whole-flow field data for a complex case study. *Build Environ* 2013;59:547-562.
235. Kubilay A, Derome D, Blocken B, Carmeliet J. Numerical simulations of wind-driven rain on an array of low-rise cubic buildings and validation by field measurements. *Build Environ* 2014;81:283-295.
236. Montazeri H, Blocken B, Hensen JLM. Evaporative cooling by water spray systems: CFD simulation, experimental validation and sensitivity analysis. *Build Environ* 2015;83:129-141.
237. Klein M. An attempt to assess the quality of large eddy simulations in the context of implicit filtering. *Flow Turbulence Combust* 2005;75:131-147.
238. Celik I, Klein M, Janicka J. Assessment measures for engineering LES applications. *J. Fluids Eng.* 2009;131:10.
239. Gousseau P, Blocken B, van Heijst GJF. Quality assessment of Large-Eddy Simulation of wind flow around a high-rise building: validation and solution verification. *Comput Fluids* 2013;79:120-133.
240. Hanna, S.R., Plume dispersion and concentration fluctuations in the atmosphere. *Encyclopedia of environmental control technology*. In: *Air Pollution Control*, Vol. 2. Houston, TX: Gulf Publishing Company, 1989;547–582.
241. Bechmann A, Sorensen NN, Berg J, Mann J, Réthoré PE. The Bolund experiment, part II: blind comparison of microscale flow models. *Bound-Layer Meteorol.* 2011;141:245-271.
242. Venturi GB. Experimental enquiries concerning the principle of the lateral communication of motion in fluids: applied to the explanation of various hydraulic phenomena. Translated from the French by Nicholson W, 1st English ed., J. Taylor, Architectural Library, High-Holborn, London; 1799.
243. ASCE Wind tunnel studies of buildings and structures. Aerospace Division of the American Society of Civil Engineers. ISBN (print): 978-0-7844-0319-8; 1999.
244. Barlow JB, Rae WH, Pope A. Low-speed wind tunnel testing. Third Edition. Wiley. ISBN: 978-0-471-55774-6; 1999.
245. Franke, J., Hirsch, C., Jensen, A.G., Krüs, H.W., Schatzmann, M., Westbury, P.S., Miles, S.D., Wisse, J.A., Wright, N.G. Recommendations on the use of CFD in wind engineering. Unpublished document, personal communication; 2004.
246. Ferziger JH, Peric M. *Computational Methods for Fluid Dynamics*, third ed. Springer, Berlin, Heidelberg, New York; 2002.
247. van Hooff T, Blocken B. On the effect of wind direction and urban surroundings on natural ventilation of a large semi-enclosed stadium. *Computers & Fluids* 2010;39:1146-1155.
248. van Hooff T, Blocken B. CFD evaluation of natural ventilation of indoor environments by the concentration decay method: CO₂ gas dispersion from a semi-enclosed stadium. *Build Environ* 2013;61:1-17

249. van Hooff T, Blocken B, van Harten M. 3D CFD simulations of wind flow and wind-driven rain shelter in sports stadia: influence of stadium geometry. *Building and Environment* 2011;46(1):22-37
250. Blocken B, van Hooff T, Aanen L, Bronsema B. Computational analysis of the performance of a venturi-shaped roof for natural ventilation: venturi-effect versus wind-blocking effect. *Comput Fluids* 2011;48(1):202-213.
251. van Hooff T, Blocken B, Aanen L, Bronsema B. Numerical analysis of the performance of a venturi-shaped roof for natural ventilation: influence of building width. *J Wind Eng Ind Aerodyn* 2012;104-106:419-427.
252. Montazeri H, Blocken B, Janssen WD, van Hooff T. CFD evaluation of new second-skin facade concept for wind comfort on building balconies: Case-study for the Park Tower in Antwerp. *Building and Environment* 2013;68:179-192.
253. Gromke CB, Blocken B, Janssen WD, Merema B, van Hooff T, Timmermans HJP. CFD analysis of transpirational cooling by vegetation: Case study for specific meteorological conditions during a heat wave in Arnhem, Netherlands. *Build Environ* 2015;83:11-26.
254. Gromke CB, Blocken B. Influence of avenue-trees on air quality at the urban neighborhood scale. Part I: Quality assurance studies and turbulent Schmidt number analysis for RANS CFD simulations. *Environmental Pollution* 2015;196:214-223.
255. Gromke CB, Blocken B. Influence of avenue-trees on air quality at the urban neighborhood scale. Part II: Traffic pollutant concentrations at pedestrian level. *Environmental Pollution* 2015;196:176-184.
256. Wieringa, J., Updating the Davenport roughness classification. *J Wind Eng Ind Aerodyn* 41-44, 357-368;1992.
257. Gromke C, Buccolieri R, Di Sabatino S, Ruck B. Dispersion study in a street canyon with tree planting by means of wind tunnel and numerical investigations – Evaluation of CFD data with experimental data. *Atmos Environ* 2008;42(37):8640-8650.
258. Mochida A, Tabata Y, Iwata T, Yoshino H. Examining tree canopy models for CFD prediction of wind environment at pedestrian level. *J Wind Eng Ind Aerodyn* 2008;96(10-11):1667-1677.
259. Melese Endalew A, Hertog M, Gebreslaise Gebrehiwot M, Baelmans M, Ramon H, Nicolai BM, Verboven P. Modelling airflow within model plant canopies using an integrated approach. *Computers and Electronics in Agriculture* 2009;66(1):9-24.
260. Moonen P, Gromke C, Dorer V. Performance assessment of Large Eddy Simulation (LES) for modeling dispersion in an urban street canyon with tree planting. *Atmos Environ* 2013;75:66-76.
261. Balczó, M., Gromke, C., Ruck, B. Numerical modeling of flow and pollutant dispersion in street canyons with tree planting, *Meteorologische Zeitschrift* 2009; 18:197-206.
262. Nikuradse J. Strömungsgesetze in rauhen Rohren. *Forsch. Arb. Ing.-Wes.* 1933;No. 361.
263. Launder BE, Spalding DB. The numerical computation of turbulent flows, *Computer Methods in Applied Mechanics and Engineering* 1974;3:269-289.
264. Cebeci T, Bradshaw P. Momentum transfer in boundary layers. Hemisphere Publishing Corporation, New York; 1977.
265. Panofsky HA, Dutton JA. Atmospheric turbulence: models and methods for engineering applications. Wiley, 397 p., 1984.
266. Karava P, Stathopoulos T, Athienitis AK. Airflow assessment in cross-ventilated buildings with operable façade elements. *Build Environ* 2011;46:266-79.
267. AIAA. Guide for the verification and validation of computational fluid dynamics simulations (G-077-1998e). 19 p.; 1998.
268. Oberkampf WL, Trucano TG. Verification and Validation in Computational Fluid Dynamics. *Progress in Aerospace Sciences*, 2002;38(3):209-272.
269. Oberkampf, W.L., Trucano, T.G., Hirsch, C., Verification, validation, and predictive capability in computational engineering and physics. *Appl. Mech. Rev.* 2004;57(5):345-384.
270. Versteeg H, Malalasekera W. An introduction to computational fluid dynamics: the finite volume method. 2nd Edition. Pearson, Prentice Hall; 2007.

Table 1. Updated Davenport-Wieringa roughness classification [256].

	z_0 (m)	Landscape description
1	0.0002 Sea	Open sea or lake (irrespective of the wave size), tidal flat, snow-covered flat plain, featureless desert, tarmac, concrete, with a free fetch of several kilometres.
2	0.005 Smooth	Featureless land surface without any noticeable obstacles and with negligible vegetation; e.g. beaches, pack ice without large ridges, morass, and snow-covered or fallow open country.
3	0.03 Open	Level country with low vegetation (e.g. grass) and isolated obstacles with separations of at least 50 obstacle heights; e.g. grazing land without windbreaks, heather, moor and tundra, runway area of airports.
4	0.10 Roughly open	Cultivated area with regular cover of low crops, or moderately open country with occasional obstacles (e.g. low hedges, single rows of trees, isolated farms) at relative horizontal distances of at least 20 obstacle heights.
5	0.25 Rough	Recently-developed “young” landscape with high crops or crops of varying height, and scattered obstacles (e.g. dense shelterbelts, vineyards) at relative distances of about 15 obstacle heights.
6	0.50 Very rough	“Old” cultivated landscape with many rather large obstacle groups (large farms, clumps of forest) separated by open spaces of about 10 obstacle heights. Also low large vegetation with small interspaces such as bush land, orchards, young densely-planted forest.
7	1.0 Closed	Landscape totally and quite regularly covered with similar-size large obstacles, with open spaces comparable to the obstacle heights; e.g. mature regular forests, homogeneous cities or villages.
8	≥ 2.0 Chaotic	Centres of large towns with mixture of low-rise and high-rise buildings. Also irregular large forests with many clearings.

Figures

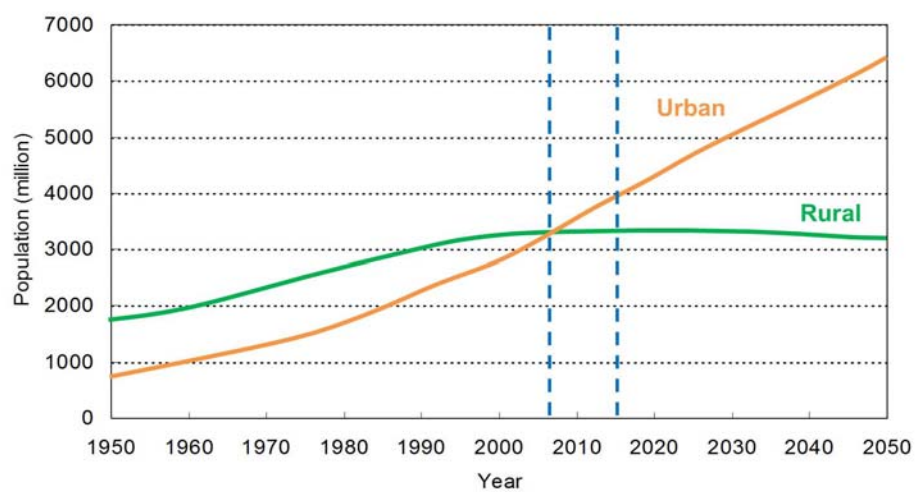


Figure 1. Urban and rural population of the world, 1950-2050 (modified from [2]).

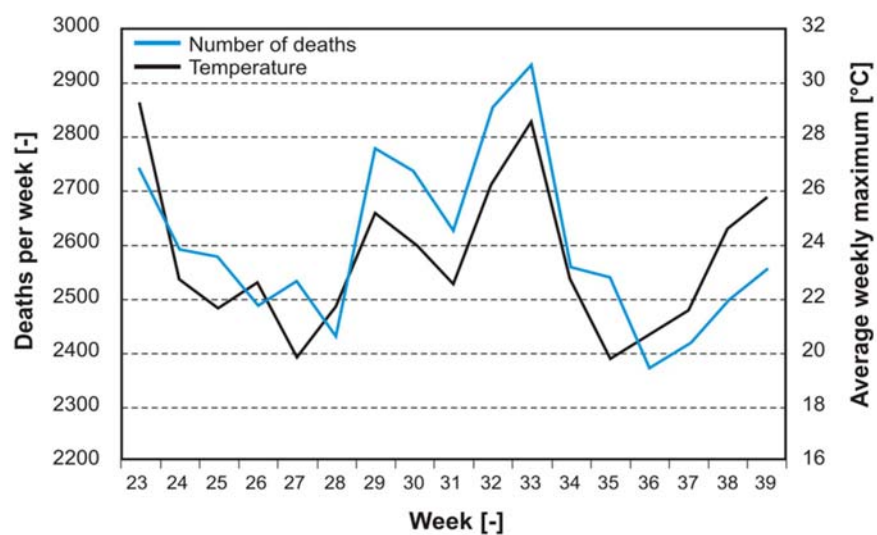


Figure 2: Mortality and average maximum outdoor air temperature per week in the Netherlands during the heat-wave period June-September 2003 (modified from [11]).

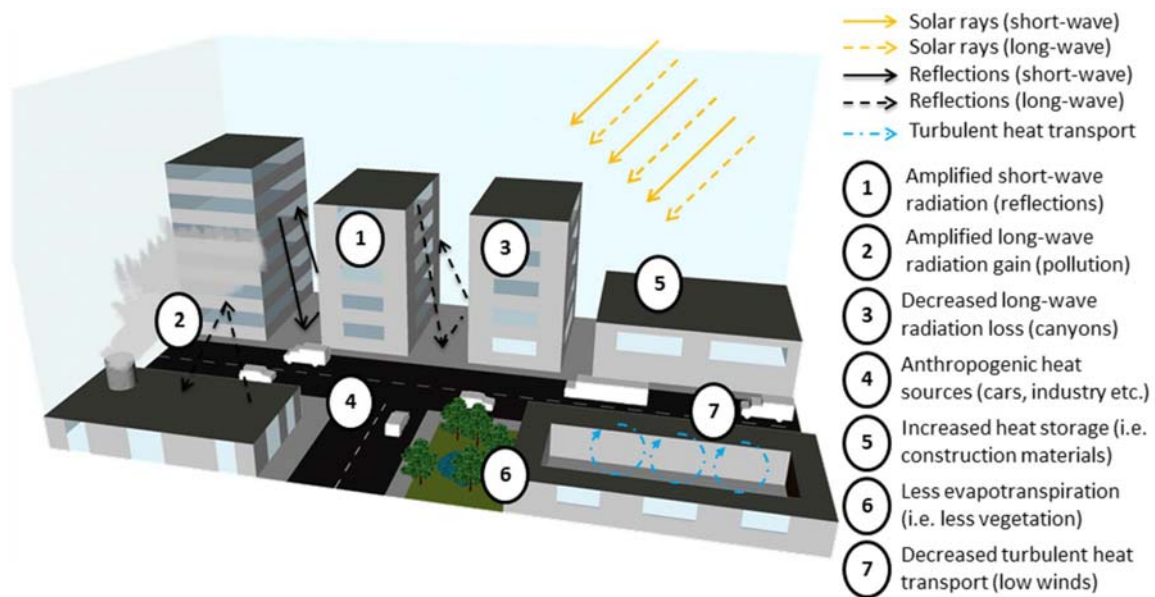


Figure 3. Causes of the urban heat island effect [19].

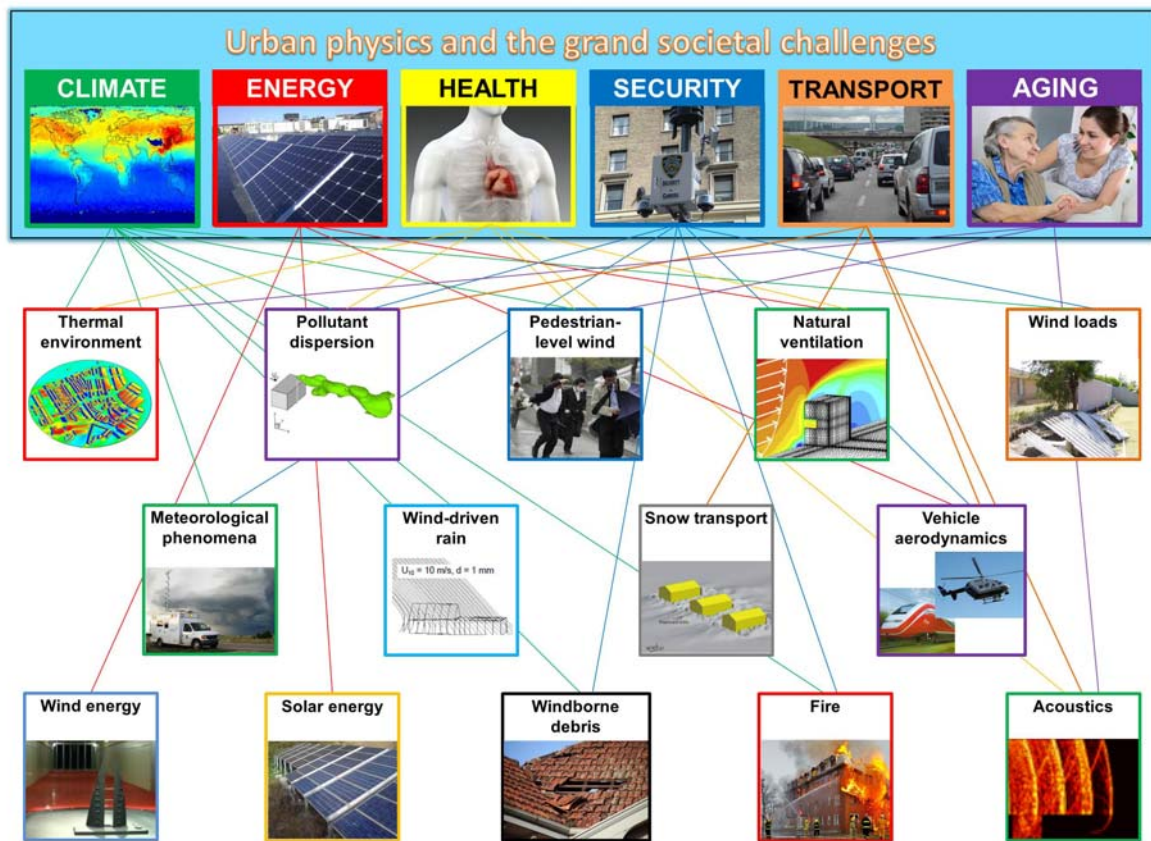


Figure 4. Link between grand societal challenges and urban physics focus areas.

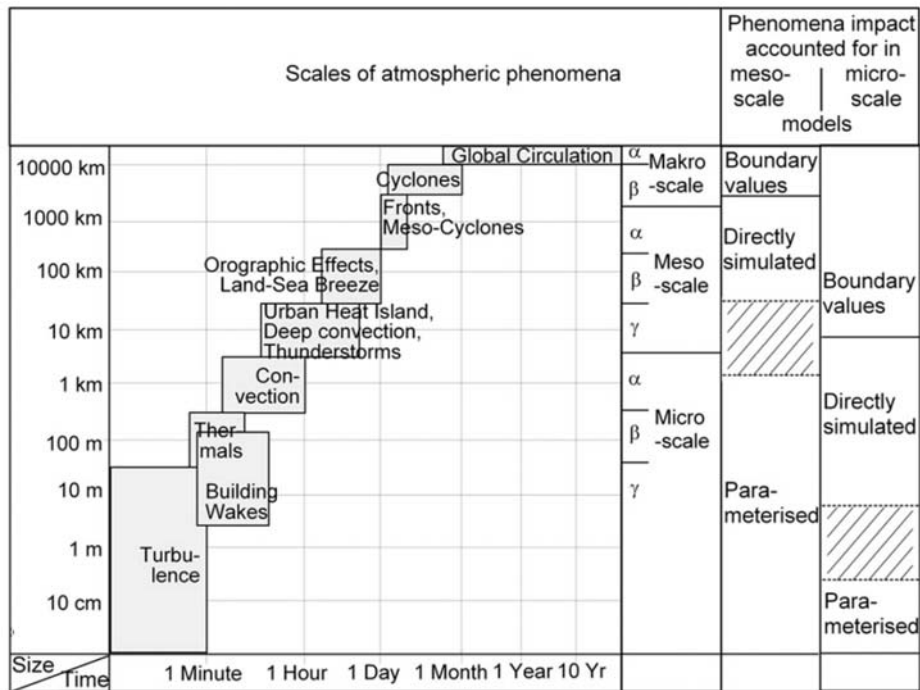


Figure 5. Spatial and temporal scales of atmospheric phenomena and how these phenomena are treated in Reynolds-averaged Navier–Stokes (RANS) mesoscale or obstacle resolving microscale models (right columns) ([130], © Elsevier), based on [131]. Dashed areas in the right columns indicate the currently used RANS model resolutions and the resulting possibly resolvable minimum phenomena sizes [130].





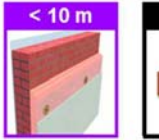
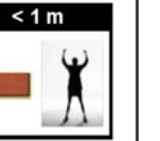
Spatial scale	Global	Mesoscale	Microscale	Building	Component	Material/Human
Distance	< 6500 km 	< 200 km 	< 2 km 	< 100 m 	< 10 m 	< 1 m 
Model cat.	NWP	NWP / MMM	CFD	CFD / BES	BC-HAM	MSM / HTM

Figure 6. Schematic representation of the six spatial scales in urban physics, their typical maximum horizontal length scales and associated model categories. NWP = Numerical Weather Prediction; MMM = Mesoscale Meteorological Model; CFD = Computational Fluid Dynamics; BES = Building Energy Simulation; BC-HAM = Building Component – Heat, Air, Moisture transfer; MSM = Material Science Model; HTM = Human Thermophysiology Model.

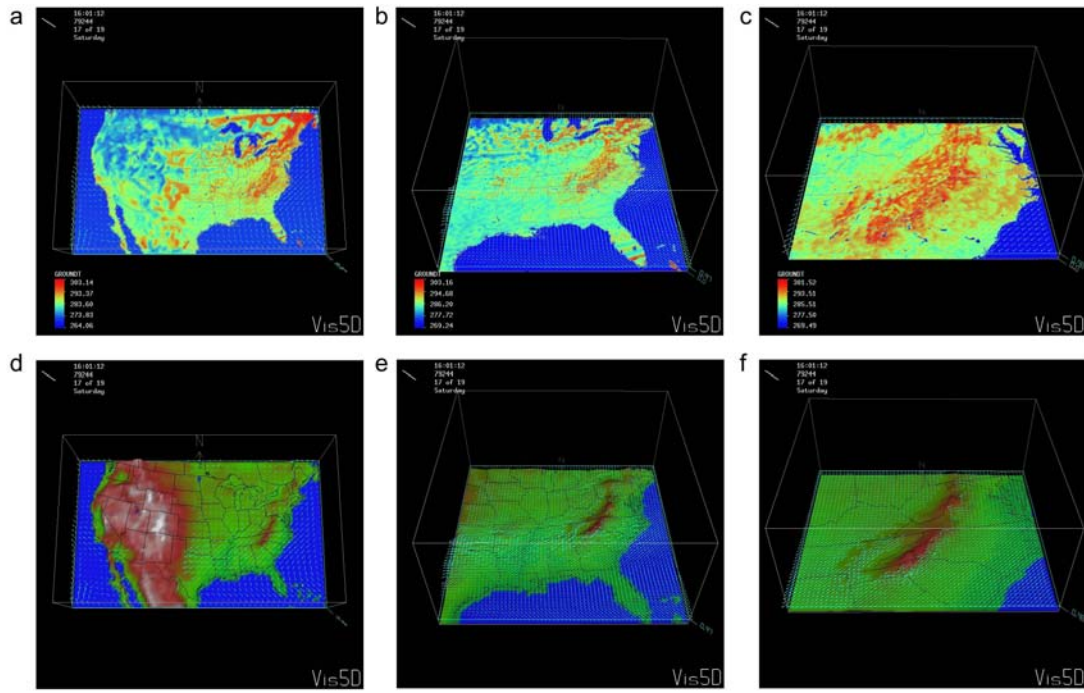


Figure 7. Results of application of the MM5 mesoscale model for (left) the continental USA, (middle) the southeastern US and (right) the Appalachian region in a nested grid configuration with three domains at resolutions of 27 km, 9 km and 3 km [144]. Figs. a-c show the ground temperature and wind vectors for domains 1, 2 and 3 at 16:01:12 GMT on Sept. 1, 1979, and Figs. d-f show the topography and wind vectors for the same three domains and the same time (from [144]).

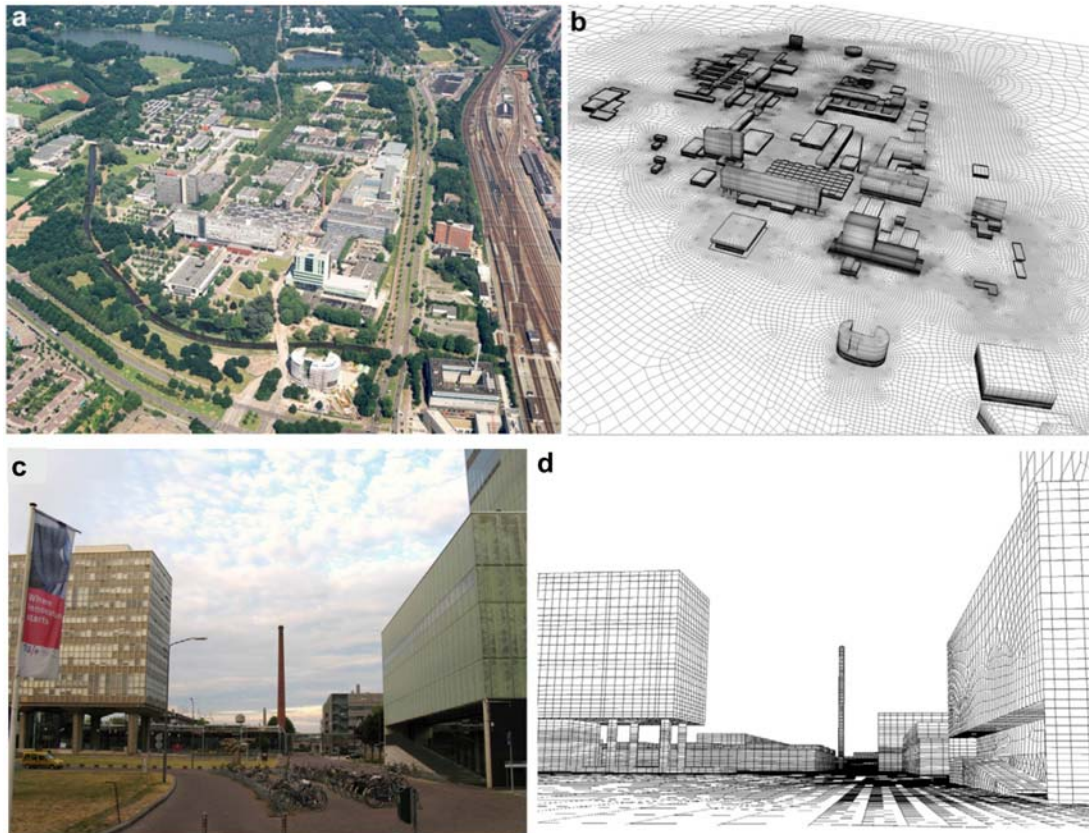


Figure 8. (a,b) Photograph and corresponding computational grid of the campus of Eindhoven University of Technology in the Netherlands for CFD simulations of wind conditions for pedestrians [49]. (c,d) Detail photograph and corresponding part of the computational grid [49].

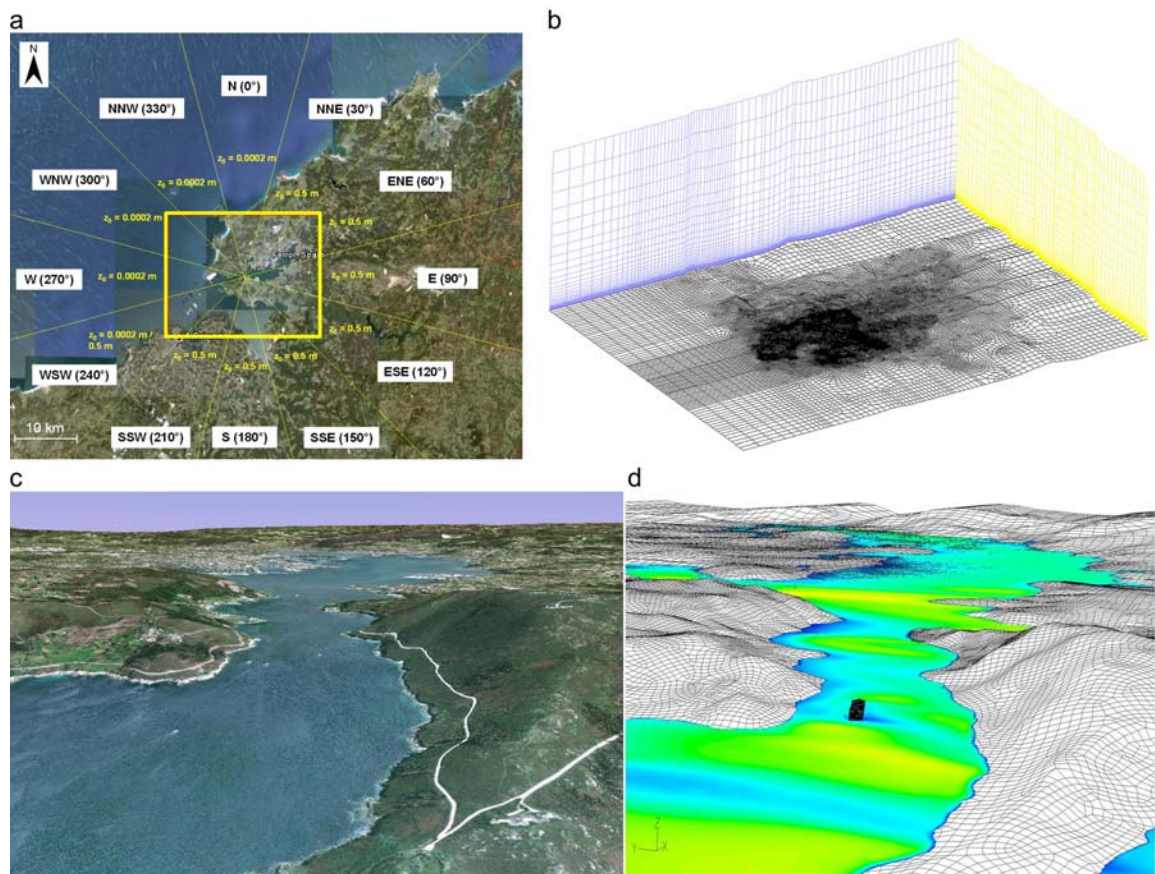


Figure 9. CFD study of wind environmental conditions in the narrow entrance channel Ria de Ferrol, Galicia, Spain. (a) Top view with indication of computational domain (yellow rectangle). (b) Computational domain with grid on bottom surface and two vertical side planes. (c) View of Ria from west. (d) View of computational grid and velocity contours of Ria from west.

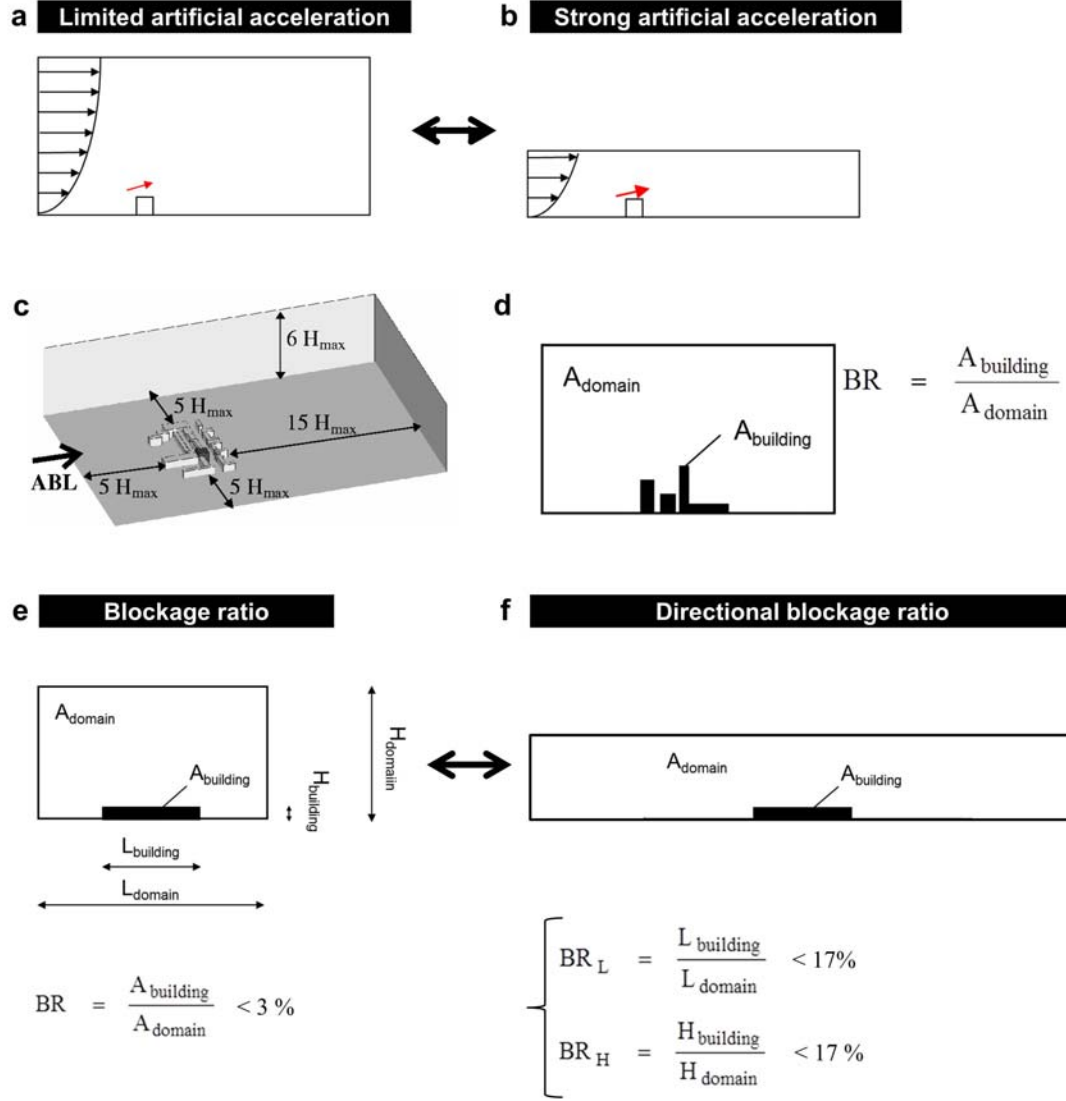


Figure 10. (a,b) Schematic representation of vertical cross-sections of a computational domain and building with only limited and with strong artificial acceleration. (c) Type-1 guidelines by Franke et al. [96] for size of computational domain (figure from [245]). (d) View in streamwise direction of building models in computational domain and definition of blockage ratio. (e) Low-rise wide building in a computational domain that satisfies existing best practice guidelines but that will give rise to artificial acceleration on lateral sides. (f) Same building in a computational domain defined based on new concept of directional blockage ratio.

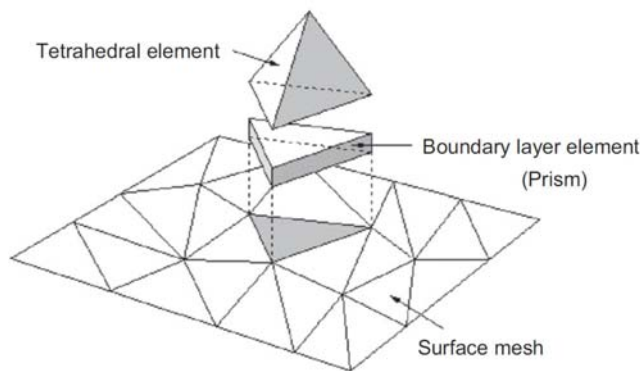


Figure 11. Arrangement of grid cells or elements near a solid surface in an unstructured grid as advised by Tominaga et al. [98].

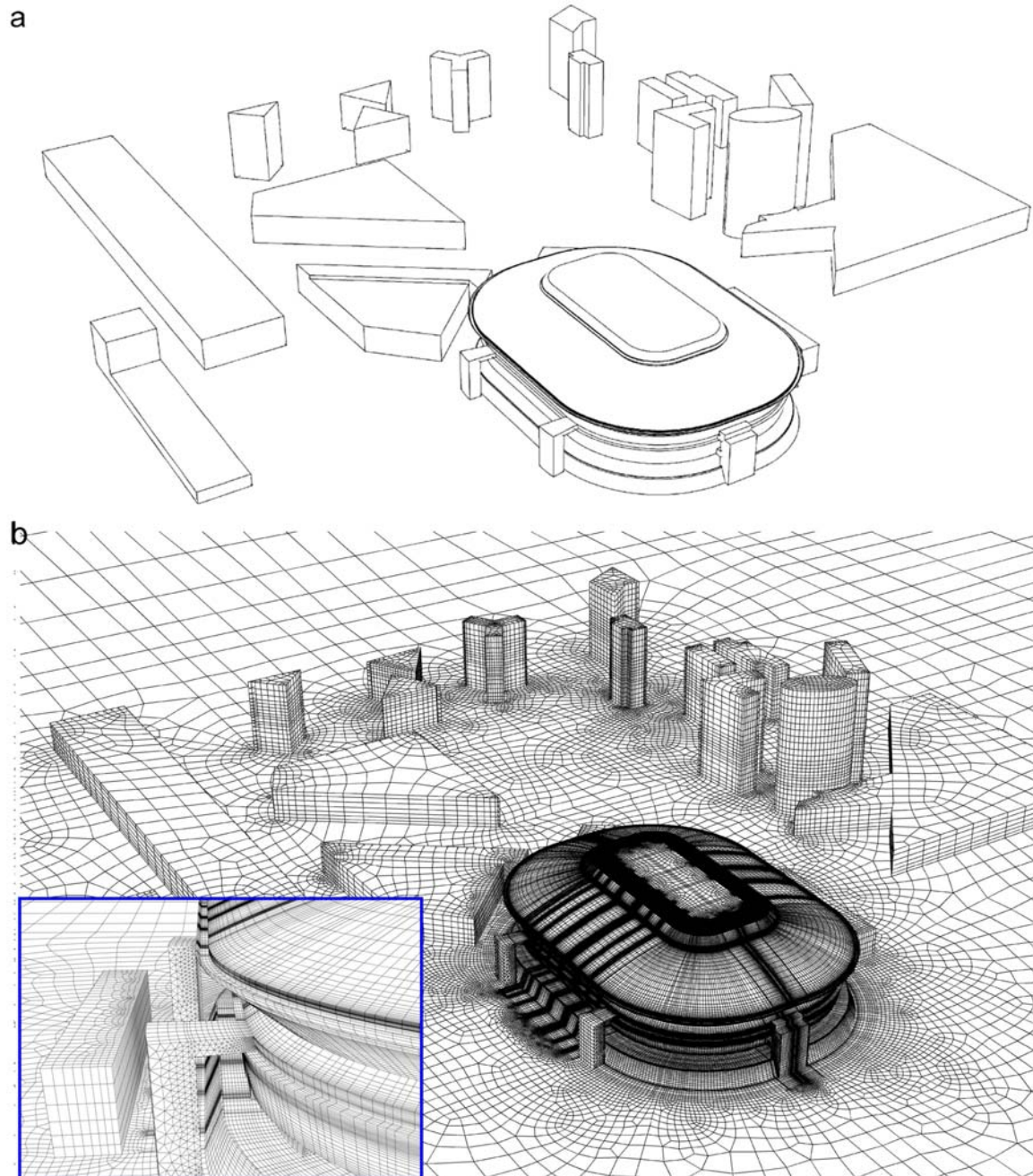


Figure 12. CFD model of Amsterdam ArenA football stadium. (a) Computational model geometry, view from northeast; (b) High-quality computational grid on the building surfaces and part of the ground surface. The grid was generated using the surface-grid extrusion technique and consists of 5.6×10^6 prismatic cells. It contains no tetrahedral cells (modified from [220]).

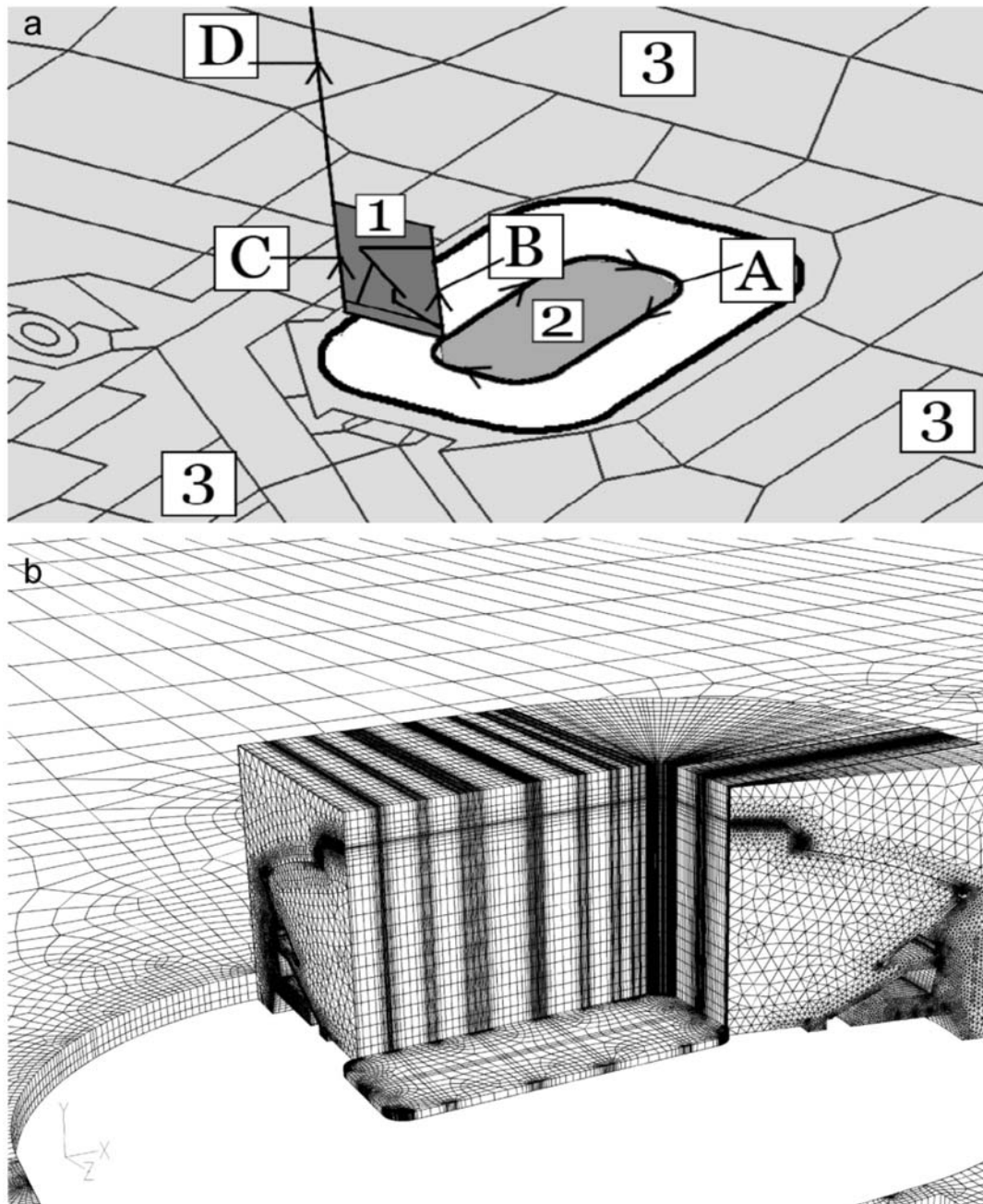


Figure 13. (a) Schematic representation of the procedure of the surface-grid extrusion technique for computational geometry and grid generation; (b) part of the grid illustrating some meshed cross-sections and resulting parts of the volume grid (from [220], © Elsevier, reproduced with permission).

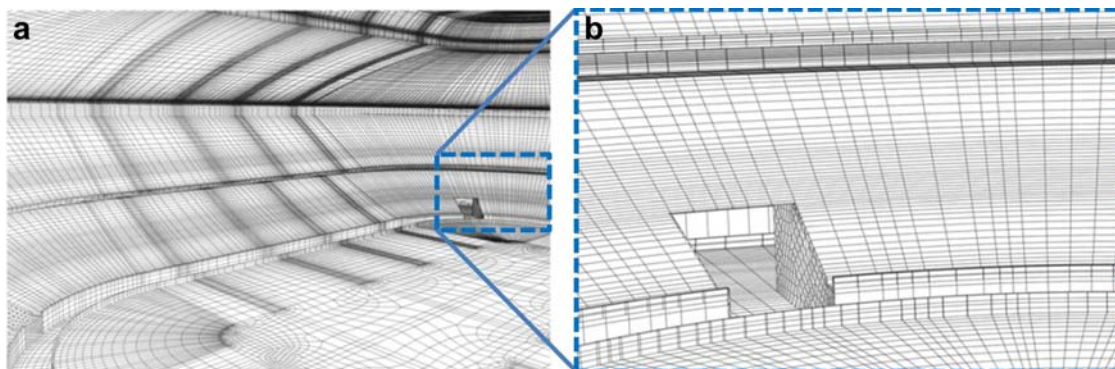


Figure 14. View of computational grid of Amsterdam ArenA football stadium from inside (modified from [248]).

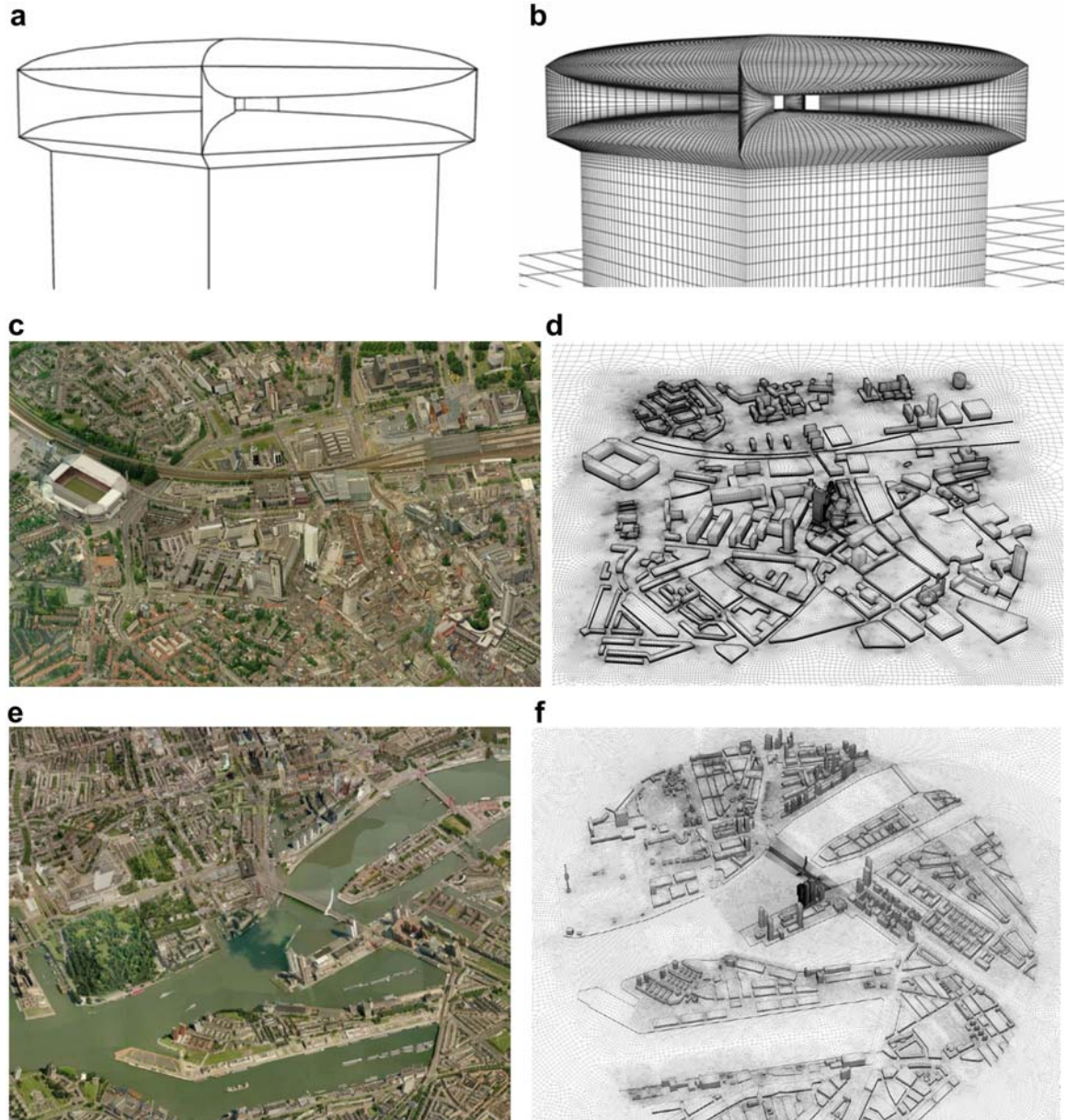


Figure 15. Computational grid of complex building or urban geometries created with the surface-grid extrusion technique. (a) Ventec roof (modified from [229]); (b) Eindhoven city center; (c) Rotterdam inner city harbor area. All three grids were made by the author's research team.

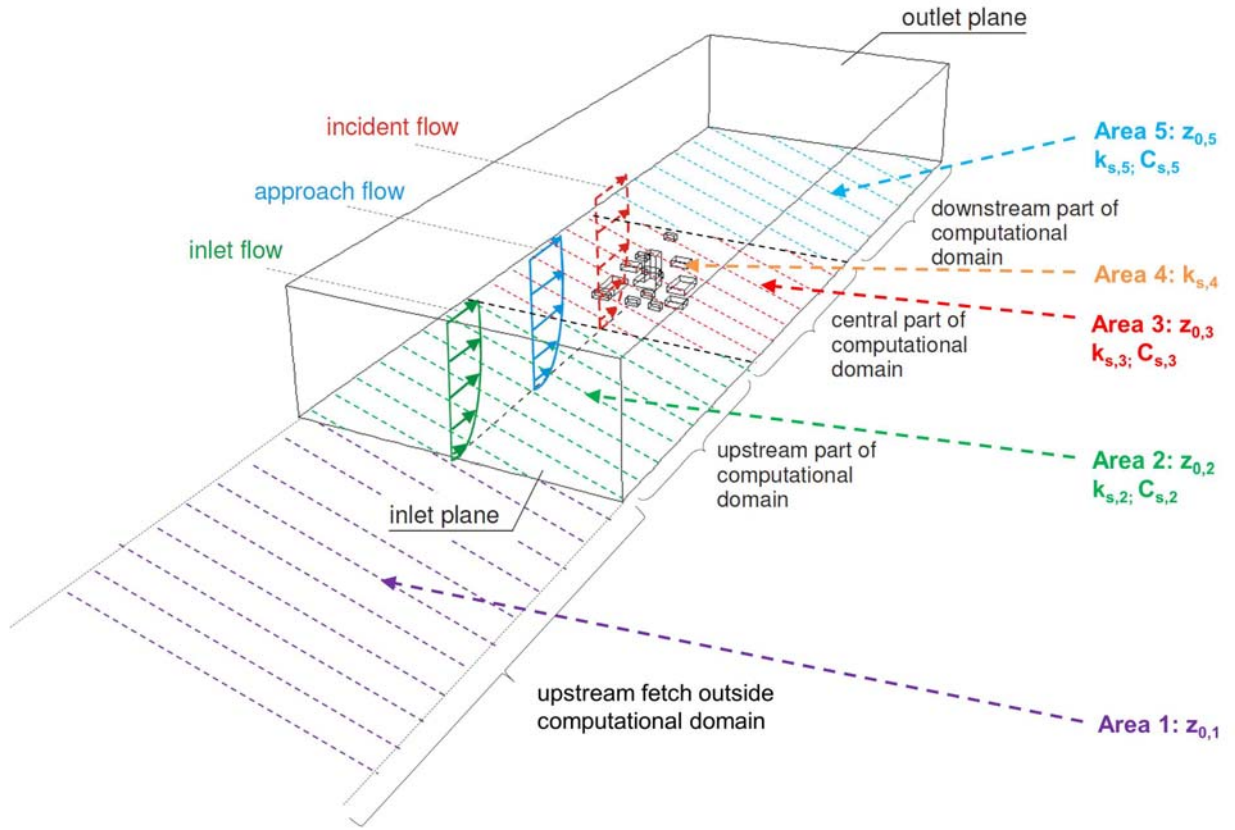


Figure 16. Schematic representation of a computational domain with four spatial areas in which roughness should be specified. Area 1 is situated outside the domain, while areas 2, 3, 4 and 5 are situated inside the domain.

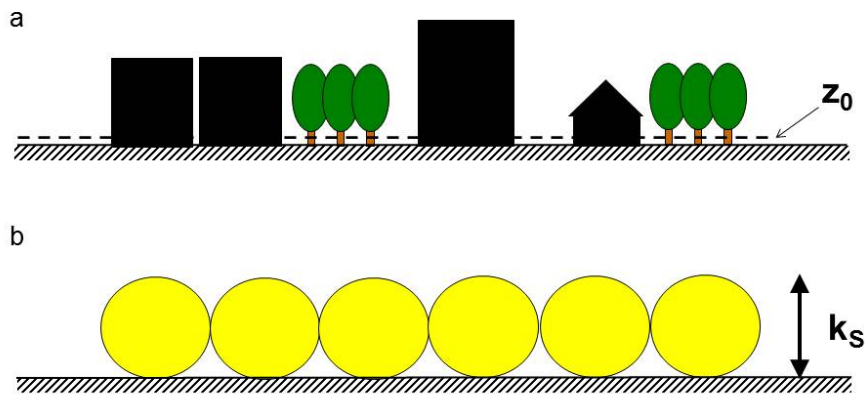


Figure 17. Schematic representation of aerodynamic roughness length z_0 and corresponding sand-grain roughness height k_s .

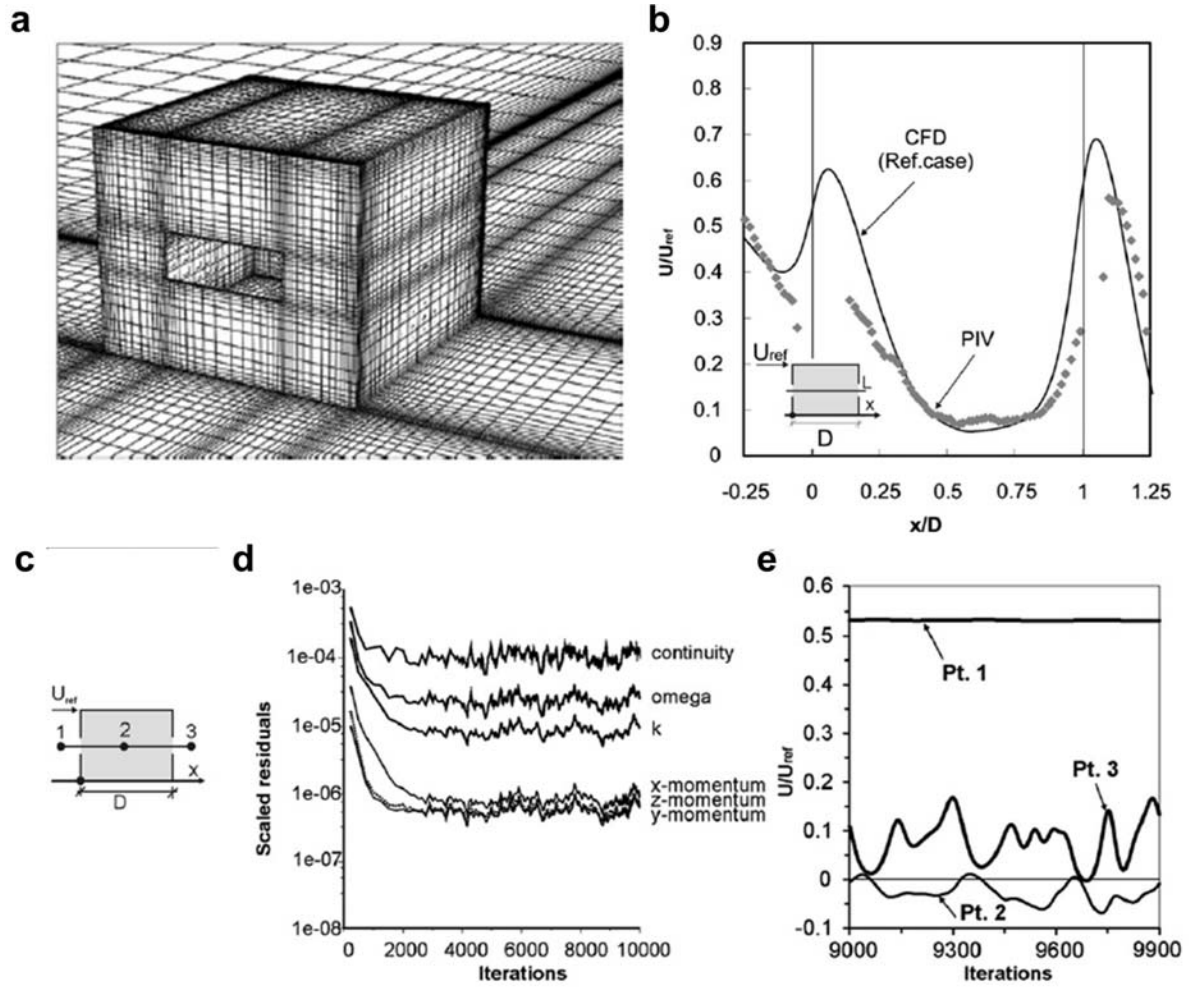


Figure 18. (a) Computational grid for generic isolated low-rise building. (b) Comparison of CFD and PIV wind speed ratio U/U_{ref} along centerline between window openings); result obtained by averaging over set of solutions at different number of iterations. (c) Position of three points along centerline. (d) Oscillatory behavior of residuals. (e) Oscillatory behavior of wind speed in points 2 and 3 (modified from [73], © Elsevier, reproduced with permission).

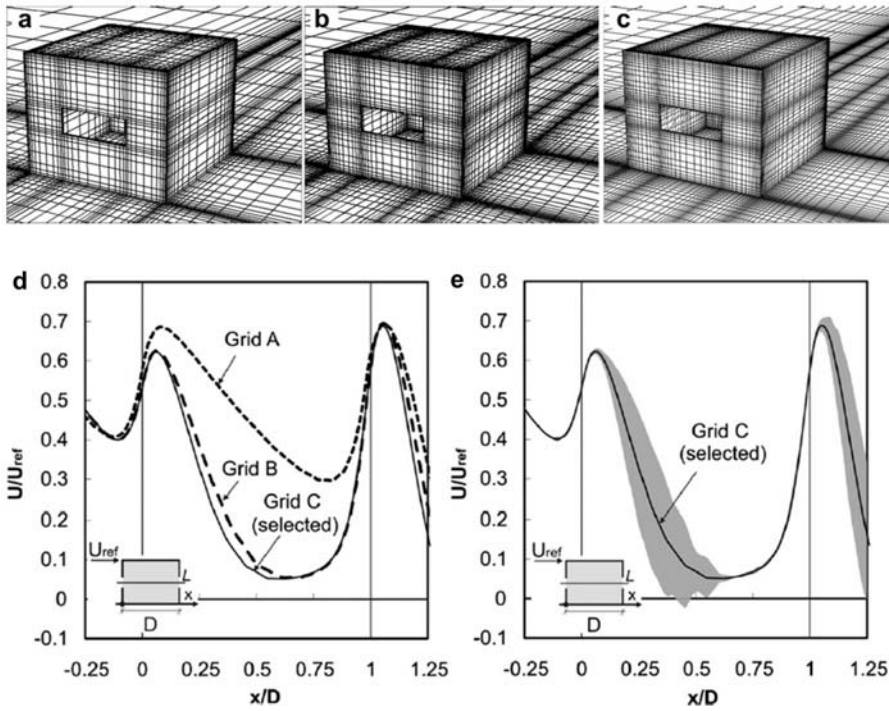


Figure 19. (a-c) Perspective view of three computational grids for grid convergence analysis: (a) coarse grid A with 144,696 cells; (b) middle grid B with 314,080 cells; (c) fine grid C with 575,247 cells (reference case). (d) Comparison of wind speed ratio U/U_{ref} along centerline through the window openings for the three grids. (e) Result on grid C with indication of band of $1.25 \times$ Grid Convergence Index by Roache [200,201]. (modified from [73], © Elsevier, reproduced with permission).